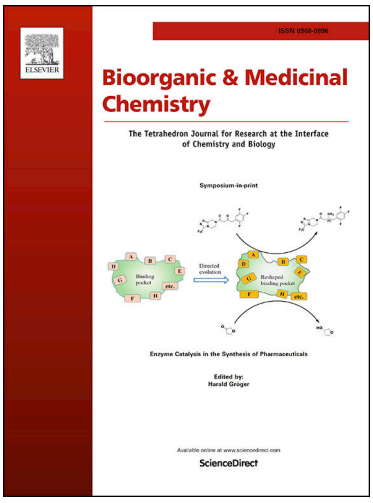

N-(Methyloxycarbonyl)thiophene sulfonamides as high affinity AT2 receptor ligands

Johan Wannberg, Johan Gising, Jens Lindman, Jessica Salander, Hugo Gutiérrez-de-Terán, Hanin Ablahad, Selin Hamid, Alfhild Grönbladh, Iresha Spizzo, Tracey A Gaspari, Robert E Widdop, Anders Hallberg, Maria Backlund, Anna Leśniak, Mathias Hallberg, Mats Larhed

PII: S0968-0896(20)30689-1
DOI: https://doi.org/10.1016/j.bmc.2020.115859
Reference: BMC 115859

To appear in: *Bioorganic & Medicinal Chemistry*

Received Date: 16 September 2020
Revised Date: 29 October 2020
Accepted Date: 31 October 2020

Please cite this article as: J. Wannberg, J. Gising, J. Lindman, J. Salander, H. Gutiérrez-de-Terán, H. Ablahad, S. Hamid, A. Grönbladh, I. Spizzo, T.A. Gaspari, R.E. Widdop, A. Hallberg, M. Backlund, A. Leśniak, M. Hallberg, M. Larhed, *N*-(Methyloxycarbonyl)thiophene sulfonamides as high affinity AT2 receptor ligands, *Bioorganic & Medicinal Chemistry* (2020), doi: https://doi.org/10.1016/j.bmc.2020.115859

N-(Methyloxycarbonyl)thiophene sulfonamides as high affinity AT2 receptor ligands

Johan Wannberg[1], Johan Gising[2], Jens Lindman[2], Jessica Salander[3], Hugo Gutiérrez-de-Terán[3], Hanin Ablahad[4,5], Selin Hamid[4,5], Alfhild Grönbladh[4], Iresha Spizzo[5], Tracey A Gaspari[5], Robert E Widdop[5], Anders Hallberg[6], Maria Backlund[7], Anna Leśniak[8], Mathias Hallberg[4], Mats Larhed[1]*

1 Department of Medicinal Chemistry, Science for Life Laboratory, BMC, Uppsala University, Box 574, SE-751 23 Uppsala, Sweden
2 The Beijer Laboratory, Department of Medicinal Chemistry, Uppsala University, BMC, Box 591, 751 24 Uppsala, Sweden
3 Department of Cell and Molecular Biology, BMC, Box 596, Uppsala University, SE-751 24, Uppsala, Sweden
4 The Beijer Laboratory, Department of Pharmaceutical Biosciences, Uppsala University, BMC, Box 591, 751 24 Uppsala, Sweden
5 Department of Pharmacology and Biomedicine Discovery Institute, Monash University Clayton 3800 VIC Australia
6 Department of Medicinal Chemistry, Uppsala University, BMC, Box 574, 751 23 Uppsala, Sweden
7 Department of Pharmacy, Uppsala University, Uppsala, Sweden and Uppsala University Drug Optimization and Pharmaceutical Profiling Platform (UDOPP), Science for Life Laboratory, Uppsala, Sweden
8 Department of Pharmacodynamics, Centre for Preclinical Research and Technology, Medical University of Warsaw, Banacha 1B Str., 02-097 Warsaw, Poland

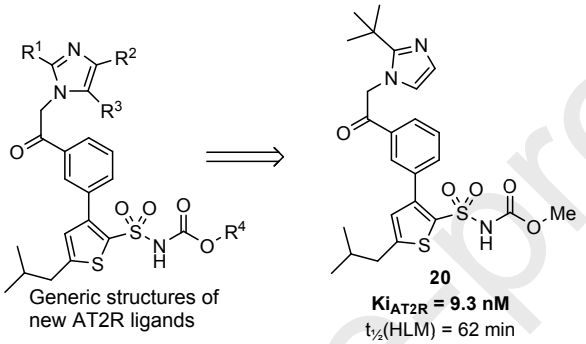

Graphical Abstract

To create your abstract, type over the instructions in the template box below.
Fonts or abstract dimensions should not be changed or altered.

Bioorganic & Medicinal Chemistry
journal homepage: www.elsevier.com

N-(Methyloxycarbonyl)thiophene sulfonamides as high affinity AT2 receptor ligands

Johan Wannberg[1], Johan Gising[2], Jens Lindman[2], Jessica Salander[3], Hugo Gutiérrez-de-Terán[3], Hanin Ablahad[4,5], Selin Hamid[4,5], Alfhild Grönbladh[4], Iresha Spizzo[5], Tracey A Gaspari[5], Robert E Widdop[5], Anders Hallberg[6], Maria Backlund[7], Anna Leśniak[8], Mathias Hallberg[4], Mats Larhed[1]*

1 Department of Medicinal Chemistry, Science for Life Laboratory, BMC, Uppsala University, Box 574, SE-751 23 Uppsala, Sweden
2 The Beijer Laboratory, Department of Medicinal Chemistry, Uppsala University, BMC, Box 591, 751 24 Uppsala, Sweden
3 Department of Cell and Molecular Biology, BMC, Box 596, Uppsala University, SE-751 24, Uppsala, Sweden
4 The Beijer Laboratory, Department of Pharmaceutical Biosciences, Uppsala University, BMC, Box 591, 751 24 Uppsala, Sweden
5 Department of Pharmacology and Biomedicine Discovery Institute, Monash University Clayton 3800 VIC Australia
6 Department of Medicinal Chemistry, Uppsala University, BMC, Box 574, 751 23 Uppsala, Sweden
7 Department of Pharmacy, Uppsala University, Uppsala, Sweden and Uppsala University Drug Optimization and Pharmaceutical Profiling Platform (UDOPP), Science for Life Laboratory, Uppsala, Sweden
8 Department of Pharmacodynamics, Centre for Preclinical Research and Technology, Medical University of Warsaw, Banacha 1B Str., 02-097 Warsaw, Poland

ARTICLE INFO

Article history:
Received
Received in revised form
Accepted
Available online

Keywords:
Angiotensin II type 2 receptor
AT2R ligands
Sulfonyl carbamates
Liver microsomes
Carboxylic acid bioisosteres

ABSTRACT

A series of meta-substituted acetophenone derivatives, encompassing *N*-(alkyloxycarbonyl)thiophene sulfonamide fragments have been synthesized. Several selective AT2 receptor ligands were identified, among those a *tert*-butylimidazole derivative (**20**) with a K_i of 9.3 nM, that demonstrates a high stability in human liver microsomes ($t_{½}$ = 62 min) and in human hepatocytes ($t_{½}$= 194 min). This methyloxycarbonylthiophene sulfonamide is a 20-fold more potent binder to the AT2 receptor and is considerably more stable in human liver microsomes, than a previously reported and broadly studied structurally related AT_2R prototype antagonist **3** (C38). Ligand **20** acts as an AT2R agonist and caused an AT2R mediated concentration-dependent vasorelaxation of pre-contracted mouse aorta. Furthermore, in contrast to imidazole derivative C38, the *tert*-butylimidazole derivative **20** is a poor inhibitor of CYP3A4, CYP2D6 and CYP2C9. It is demonstrated herein that smaller alkyloxycarbonyl groups make the ligands in this series of AT2 selective compounds less prone to degradation and that a high AT2 receptor affinity can be retained after truncation of the alkyloxycarbonyl group. Binding modes of the most potent AT_2R ligands were explored by docking calculations combined with molecular dynamics simulations.

1. Introduction

Angiotensin II (Ang II) is an important component of the renin−angiotensin system (RAS). The octapeptide acts mainly through the activation of two receptor subtypes; the AT1 receptor (AT_1R) and the AT2 receptor (AT_2R). Stimulation of AT_1R by Ang II has a major impact on blood pressure regulation and the fluid/electrolyte balance. Hence, suppression of the formation of Ang II from angiotensinogen by inhibitors of the metalloprotease angiotensin converting enzyme (ACE) or of the aspartyl protease renin or alternatively, blockade of AT_1R by angiotensin receptor antagonists (ARBs) *i.e.* the sartans are major established strategies to control blood pressure in hypertensive patients. The first ACE inhibitor captopril,[1,2] the first renin inhibitor aliskiren,[3] and the first ARB losartan **1**[4,5] were introduced onto the market in 1978, 2007 and 1995, respectively.

In recent years, several potential drug targets in RAS have been assessed in detail[6] and among those the AT2 receptor has attracted most interest and has now emerged as a new promising target for drugs[5,7–11] This receptor, in contrast to AT_1R is sparsely expressed in healthy adults but is strongly up-regulated after tissue damage[12–14] such as neuronal injury[15] and vascular injury[16] and following myocardial infarction[17–19] and brain ischemia[20,21]

The receptor very often mediates opposite actions to those resulting from AT_1R stimulation.[22,23] In recent years a large number of selective and potent AT_2R agonists have been reported.[9,24–26] The first small-molecule AT_2R agonist **2** (C21) that was discovered by Hallberg's group in our laboratories[27] has been studied extensively and demonstrated beneficial effects in a series of experimental models.[24,25] C21 is now in clinical trials aimed for idiopathic pulmonary fibrosis. Recently, it was observed that a migration of the methylene imidazole group from the *para* to *meta* position converted the AT_2R agonist **2** into an AT_2R antagonist, **3** (C38).[28] One AT_2R antagonist, the carboxylic

acid clinical trials but these trials were terminated in 2019 due to safety reasons. EMA401 that was synthesized more than twenty years ago by Parke-Davis, is structurally related to the old prototype AT_2R antagonists PD-123319 (EMA200) and PD-126055 (EMA400) and has demonstrated a good oral bioavailability (33%) in rat.[29] The antagonist **4**, which is the *S*-enantiomer of EMA400, has a very different chemical structure as compared to **3** was aimed for the management of neuropathic pain,[30–32] hence both agonists and antagonists to AT2 receptor have been examined as potential new pharmaceutical agents (Figure 1).

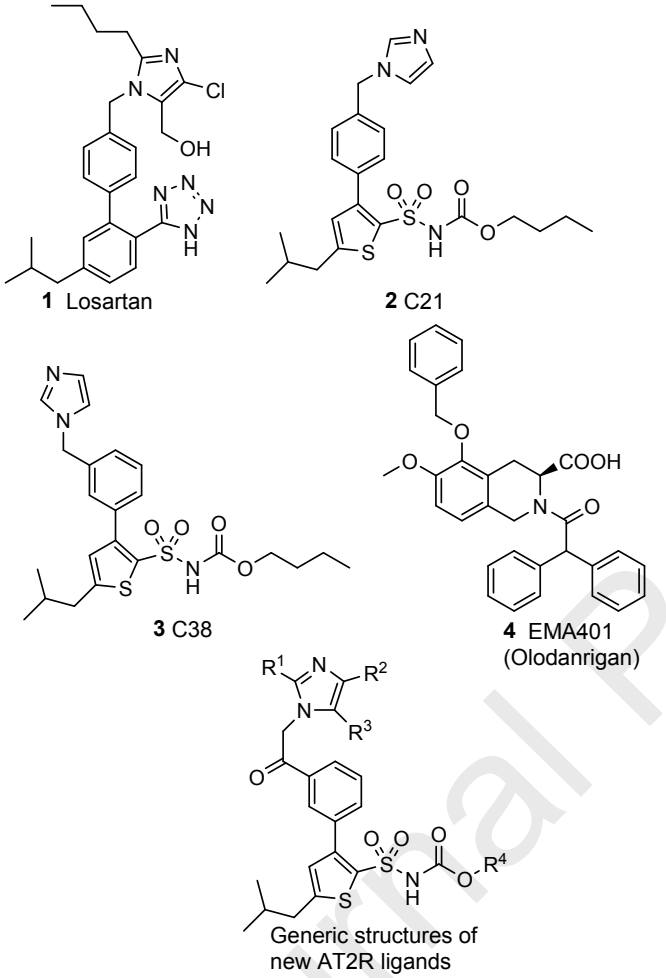

Figure 1. Ligands interacting with the AT1 receptor exemplified by the antagonist losartan (**1**) and with the AT2 receptor exemplified by the agonist C21 (**2**), the antagonists C38 (**3**) and Olodanrigan (**4**).

While comprehensive SAR has been established for AT_2R agonists related to **2** (C21), [27,33–38] very limited information is available on the impact of modifications of the AT_2R antagonist **3** on binding affinities at the AT_2R and on the metabolic stability of **3** and analogous compounds thereof, neither from *in vivo* nor *in vitro* experiments.[28,39–41] It was previously shown by our laboratories that **3** (C38) and other structurally related *meta*-substituted compounds examined, act as AT_2R antagonists in a neurite outgrowth assay. Thus, pretreatment of NG108-15 cells with the AT_2R antagonists reduced C21 (**2**)-induced and Ang II-induced neurite outgrowth.[28,42] More recently, we reported, that **3** (C38) acts as a partial agonist in an assay relying on iNOS-derived NO release in M1 phenotypic macrophages.[43]

We herein report two bioisosters of **3**, the carboxylic acid **5** and the tetrazole derivative **6.** Furthermore, we report the stability in liver human and mouse microsomes and of a series of acetophenone derivatives; the *meta*-substituted imidazolylacetylphenyl *N*-alkyloxycarbonyl sulfonamides **7-23** and the *N*-acetylsulfonamide **24** (Scheme 2 and 3). High affinity, receptor selective ligands exhibiting favorable *in vitro* ADME profiles were identified.

2. Chemistry

The carboxylic acid derivative **5** was prepared by a lithiation/borylation/esterification/Suzuki coupling sequence where 5-isobutylthiophene-2-carboxylic acid was converted to the 3-boronic acid-2-ethyl ester and then coupled to 1-(3-bromobenzyl)-1H-imidazole to give **5** after ester hydrolysis. The tetrazole compound **6** was prepared by Suzuki coupling of (2-(tert-butylcarbamoyl)-5-isobutylthiophen-3-yl)boronic acid[33] and 1-(3-bromobenzyl)-1H-imidazole followed by removal of the *t*Bu group and dehydration of the primary amide to the nitrile and finally cycloaddition with sodium azide as shown in Scheme 1.

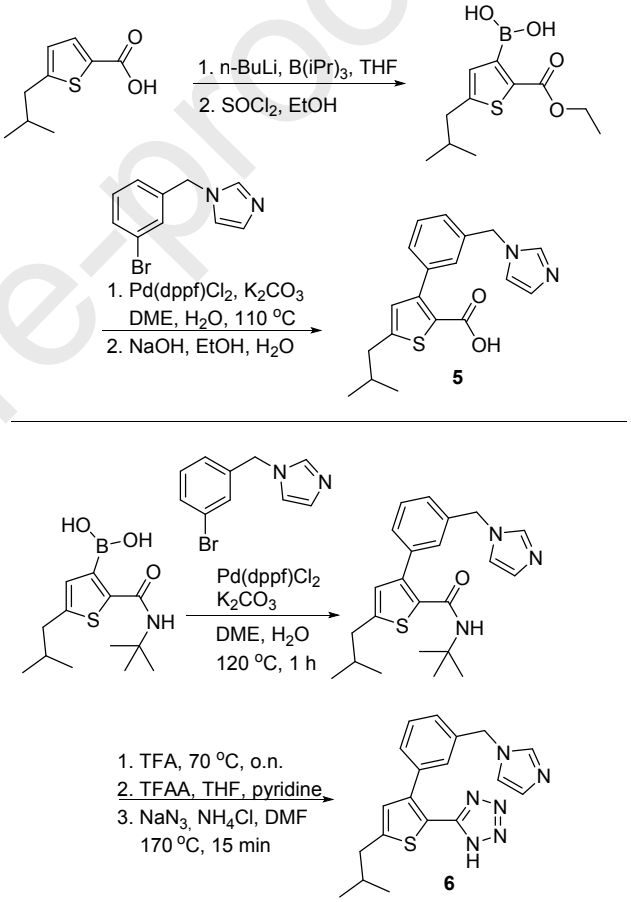

Scheme 1. Synthesis of the carboxylic acid and tetrazole analogs of C38

The MIDA boronate, 2-(*N*-(*tert*-butyl)sulfamoyl)-5-isobutylthiophen-3-yl)boronic acid MIDA ester, was prepared as previously described[39]. The synthesis of butylsulfonylcarbamates, **7-19** was initiated by *N*-alkylation of the appropriate imidazoles and benzimidazoles with 2,3′-dibromoacetophenone to deliver the alkylated intermediates in moderate to high yields (Scheme 2). These were then applied to Suzuki couplings with the MIDA boronate to deliver thienylphenyl intermediates. The compounds were further treated with TFA to deprotect the *N*-*tert*-butyl sulfonamide function and subsequently the primary sulfonamides were reacted with butyl chloroformate to furnish the desired

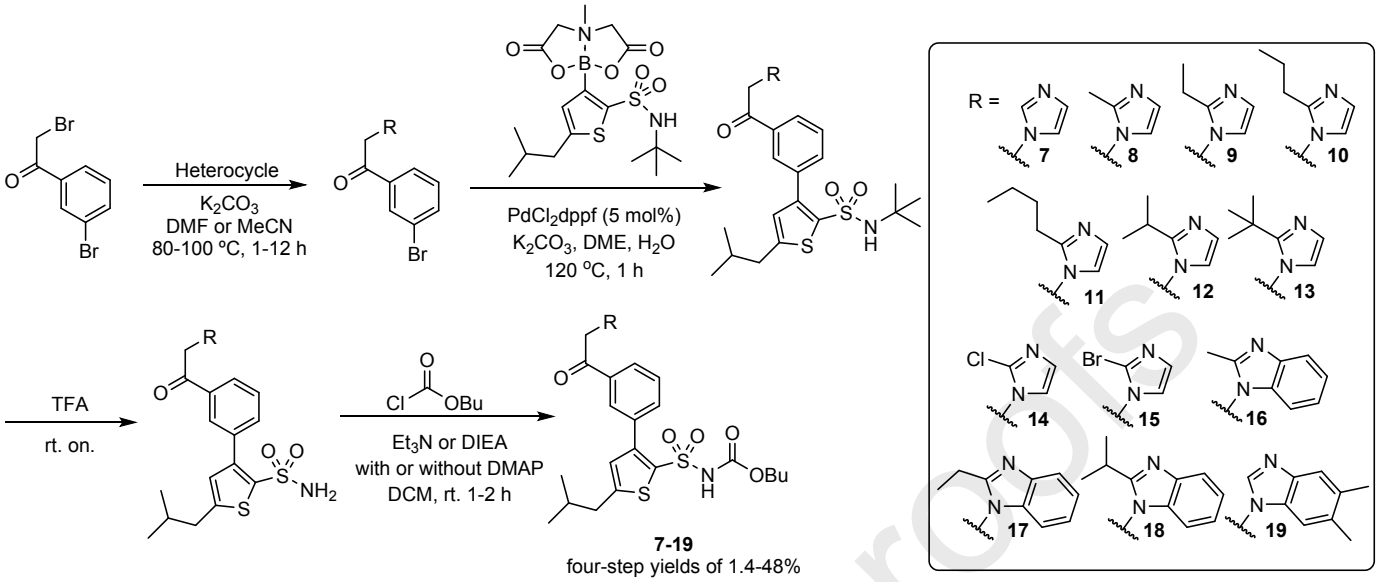

Scheme 2. Synthesis of the compounds **7**-**19**.

The primary sulfonamide containing the 2-*tert*-butylimidazolyl moiety was treated with methyl chloroformate at room temperature to give ligand **20** in 39% yield over three steps and a primary sulfonamide containing the 2-cyclopropylimidazolyl moiety was treated with methyl- and ethyl chloroformate to give the corresponding carbamates **21** and **22** (Scheme 3). Analogous to a previously described methodology,[39,44] compound **13** was heated in ethanol at 100 °C for 30 min in a closed vessel to give **23** in 49% yield. Finally a primary sulfonamide was treated with acetyl chloride to give the acyl sulfonamide **24** in 57% yield.

3. Biological evaluation

In the present report, a binding assay using membrane preparations from HEK-293 cells expressing human AT_2R (HEK293-hAT_2R) and that relies on displacement of the non-selective AT_2R/AT_1R ligand sarile ([^{125}I][Sar^1,Ile^8]-angiotensin II) using a seven-point dose-response curve in duplicate measurements at each concentration was applied (Eurofins Cerep SA, France). The imidazole compound **3** resulted in a K_i value of 270 nM[39] Prior to initiating a more extensive medicinal chemistry program we felt prompted to first assess two alternative and more common acidic functions as alternatives to the butoxy sulfonyl carbamate group of **3**. However, neither the carboylic acid **5** nor the tetrazole derivatives **6** displayed any notable affinity to AT2R.

The prototype AT_2R antagonist compound **3** was previously reported to exhibit a K_i value of 19 nM and the acetophenone derivative **7** comprising an imidazole heterocycle attached by a methylene bridge to the *meta* position, a K_i of 22 nM.[28] These affinity data were obtained from a radioligand assay built on displacement of [^{125}I]Ang II from AT2 receptors in membrane preparations from pig uterus myometrium.[45,46] In the HEK293-hAT2R assay applied in this report the acetophenone derivative **7** exhibited a K_i of 280 nM (Figure 2). Thus, an approximately 10-fold lower affinity was encountered in the HEK293-hAT_2R membrane assay using the peptide ligand sarile, that like Ang II acts as a AT_2R agonist.[47]

Furthermore, we previously reported that a reduced ketone function of compound **7** resulted in compound exhibiting a 5-fold lower affinity, suggesting an importing role of the carbonyl oxygen.[25] We knew from studies of the C21 AT_2R agonist series that substituents at the imidazole ring system tended to limit the interaction with CYP450 enzymes.[35] This information prompted us therefore to attach various alkyl substituents of different size at the 2-position of the imidazole ring moiety.

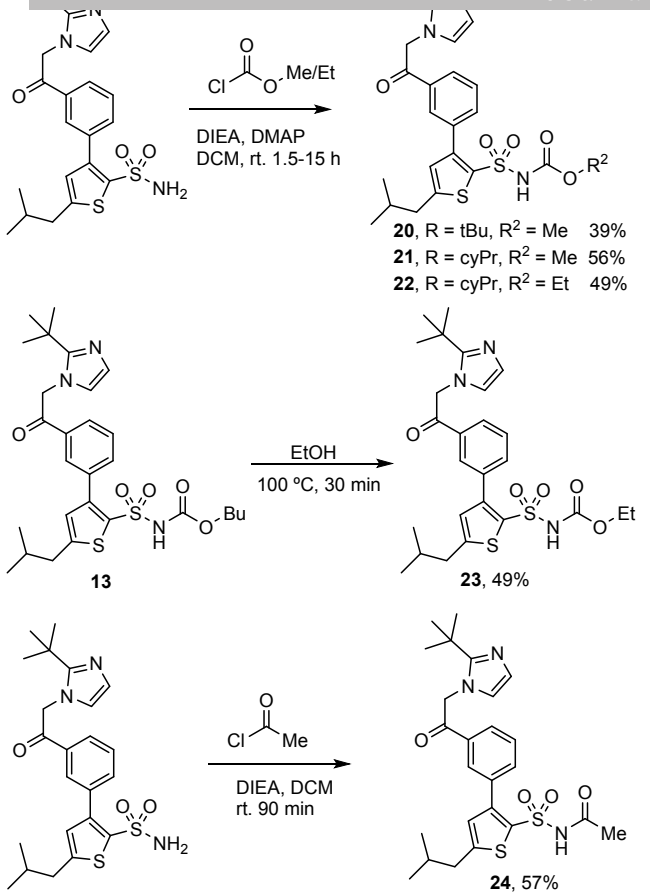

As demonstrated in Figure 2 a significant improvement of the binding affinity to the AT2 receptor could be achieved. Small bulky groups like an isopropyl or a *tert*-butyl group in the 2-position rendered the highest affinities. Compound **12** exhibited a K_i value of 17 nM and compound **13** a K_i of 6.6 nM. Hence a 50-fold improvement of the affinity to the AT2 receptor could be accomplished by this maneuver.

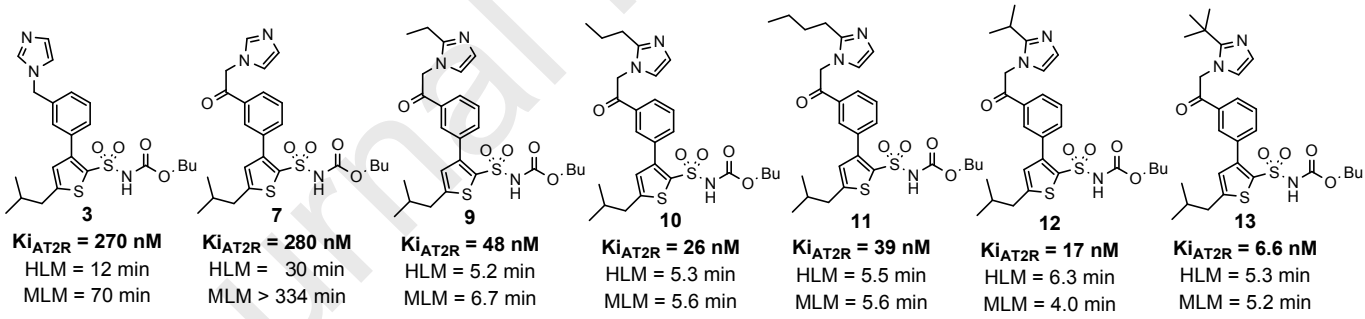

Regarding stability of the compounds in liver microsomes, whilst **4** (EMA401) and the AT_2R agonist **2** (C21), in the assay we applied exhibited good to fair *in vitro* stability in human liver microsomes, $t_{½}$= 38 min and 22 min, respectively, the AT_2R antagonist **3** that is structurally related to **2**, demonstrated a considerably lower stability, $t_{½}$= 12 min.[39] More encouraging, as described herein the acetophenone derivative **7** that is essentially equipotent to **3** regarding AT_2R affinity displayed a substantial improvement regarding the stability in human liver microsomes (HLM) with a half-life of 30 min. Unfortunately, the 15-fold more potent compound **12** encompassing the acetophenone linker, suffers from very poor *in vitro* metabolic stability (HLM $t_{½} \leq 6.3$ min). Similarly, the *tert*-butyl derivative **13** that is a 40 times more potent than **7** as an AT_2R binder decomposes fast in the human liver microsome assay (HLM $t_{½} \leq 5.3$ min). Thus, it seems obvious that considering the fast metabolism also in mouse microsomes (MLM $t_{½} < 6$ min) that the compounds *e.g.* **12** and **13** are not suitable for experiments using mice in pain models.

A series of ligands were synthesized to probe whether the stability in microsomes could be improved with the butyloxycarbonyl functionality intact but by replacing the imidazole group with other functionalities. Neither of the compounds **8**, **14-19**, with a possible exception of **19** demonstrated any significantly improved stability in human or mouse liver microsomes (Figure 3).

As deduced from SAR studies of a series of AT_2R agonists, the *n*-butyl group seemed optimal for binding to the activated form of the receptor.[48] However, regarding AT_2R antagonists, structural variations of the lipophilic side chain was tolerated by the receptor.[39] Furthermore, the methoxycarbonyl analogue of **3** (C38) was reported to be considerably less prone to decomposition in both mouse and human microsome assays (MLM = 220 min; HLM = 77 min).[39] As a consequence of these findings we decided to retain the *tert*-butyl group attached at the imidazole heterocycle to hopefully maintain a high affinity to AT_2R whilst reducing lipophilicity of the ligands by shorten the *n*-alkyloxycarbonyl chain. A combination of a *tert*-butyl group attached to the imidazole heterocycle of the parent acetophenone derivative **7** with a K_i of 280 nM and a methyloxycarbonyl rather than a butyloxycarbonyl group rendered **20** with a K_i of 9.3 nM. An ethoxycarbonyl instead of a methyloxycarbonyl group provided ligand **23** exhibiting a K_i of 7.6 nM (Figure 4). A significant improvement of the metabolic stability was observed for the methyloxycarbonyl group (**20**) compared to the ethyloxycarbonyl (**23**). Ligand **20** exhibited a stability in the HLM assay ($t_{½}$ = 62 min) that was superior to what had been monitored with any other compound in the series and a high

sulfonyl carbamate group

Figure 2. Binding affinities (K_i) to the AT2 receptor (human HEK-293 cells) and stability ($t_{½}$ in minutes) in human liver microsomes (HLM) and mouse liver microsomes (MLM) of the butyloxycarbonyl sulfonamides **3**, **7**, **9-13**.

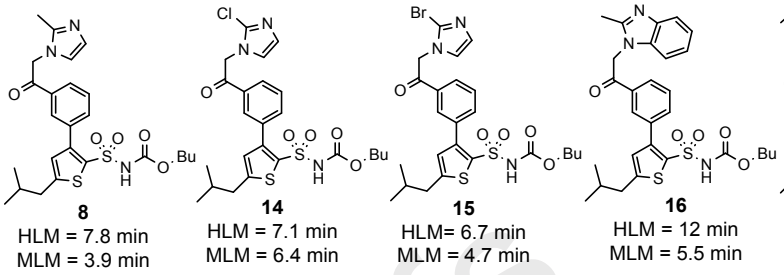

Figure 3. The stability of the butyloxycarbonyl sulfonamides **8**, **14-19** ($t_{½}$ in minutes) in human liver microsomes (HLM) and in mouse liver microsomes (MLM).

metabolic stability of **20** in liver microsomes from mice was much poorer ($t_{½}$ = 16 min). A displacement of the *tert*-butyl group of the potent ethyloxycarbonyl compound **23** for a cyclopropyl group resulted in **22** that was a significantly poorer binder to AT_2R than **23**, although the metabolic stability of the compound in the HLM assay (**22**: $t_{½}$= 36 min versus for **23**: $t_{½}$ = 21 min) and in human hepatocytes (**22**: $t_{½}$ = 79 min versus for **23**: $t_{½}$ = 43 min) was improved. The cyclopropyl methyloxycarbonyl sulfonamide **21** was the most inert compound in the HLM assay of all derivatives assessed ($t_{½}$ = 114 min). Furthermore, this cyclopropyl compound (**21**) is also the most stable compound in human hepatocytes, with a $t_{½}$ of 280 min. The acetylsulfonamide **24** exhibited a more than 15-fold higher K_i value than the methyloxycarbonyl derivative **20** and in addition, it exhibited a lower stability in the HLM assay and in human hepatocytes $t_{½}$= 36 min and 40 min, respectively. However, the acetylsulfonamide **24** is still more metabolically stable than **3** and exhibits a considerably better K_i value than both **3** and the parent acetophenone compound **7**. (Figure 4).

The potent methoxycarbonyl derivative **20** neither inhibits CYP3A4 (IC_{50} ~50 µM), CYP2D6 (IC_{50} > 50 µM) nor CYP2C9 (IC_{50} > 15 µM) significantly. This is in sharp contrast to **2** (C21), which comprises a unsubstituted imidazole heterocycle as a characteristic element and with a HLM half-life of 22 min. Imidazole derivatives like **2** that are high affinity AT_2R agonists are often associated with a pronounced capacity to inhibit CYP enzymes.[35] The ability of the prototype AT_2R antagonist **3** (C38) to inhibit important CYP isoenzymes was therefore examined. This imidazole compound, exhibiting a K_i value of 280 nM at the AT2 receptor was indeed found to act as an exceptionally potent inhibitor of the three common drug-metabolizing CYP enzymes assessed.

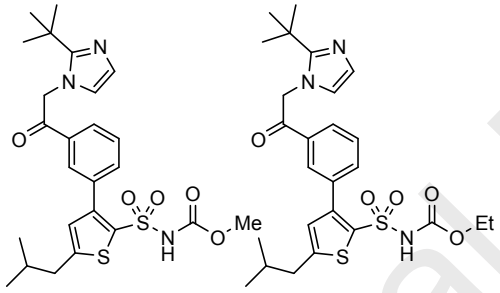

20
Ki_{AT2R} = 9.3 nM
HLM = 62 min
MLM = 16 min

23
Ki_{AT2R} = 7.6 nM
HLM = 21 min
MLM = 11 min

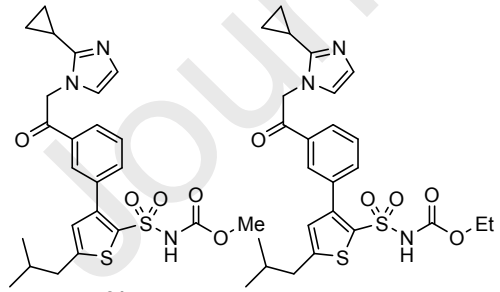

21
Ki_{AT2R} = 110 nM
HLM = 114 min
MLM = 58 min

22
Ki_{AT2R} = 53 nM
HLM = 36 min
MLM = 35 min

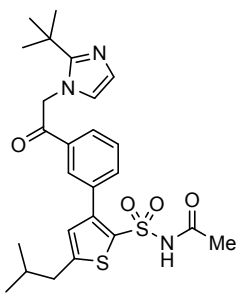

24
Ki_{AT2R} = 170 nM
HLM = 36 min
MLM = 72 min

cells and stability ($t_{½}$ in minutes) in human liver microsomes (HLM) and mouse liver microsomes (MLM) of the ethyloxycarbonyl and methyloxycarbonyl sulfonamides **20**-**23** and of the acetylsulfonamide **24**.

The following data were recorded; CYP3A4; IC_{50} ~120 nM, CYP2D6; IC_{50} 2 µM and remarkably CYP2C9; IC_{50} < 100 nM.

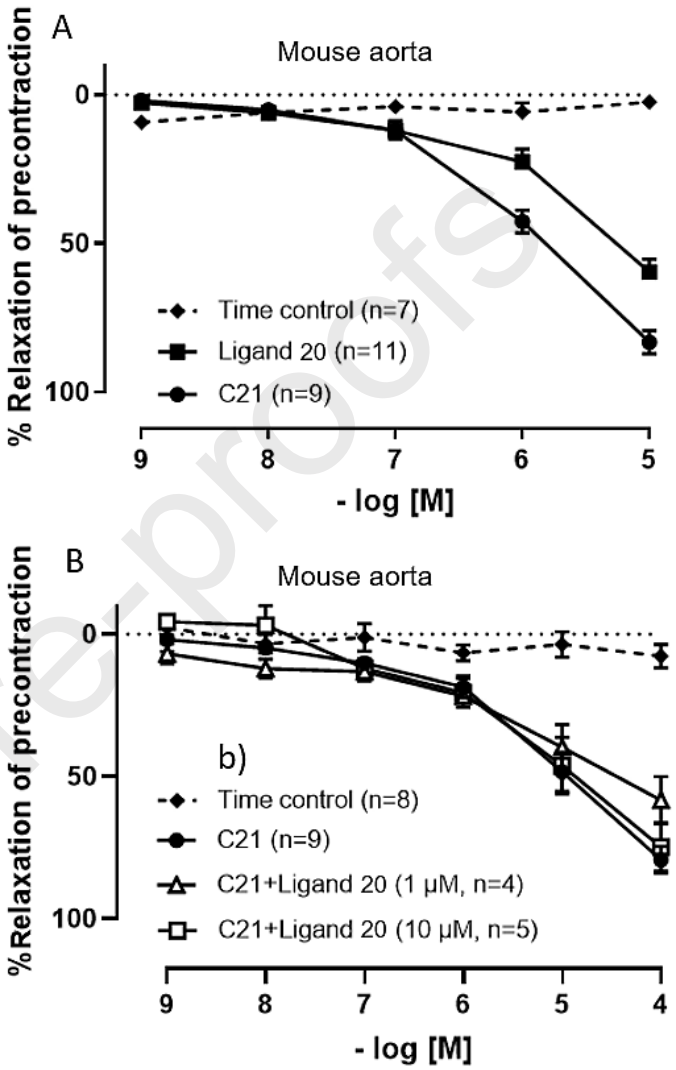

Figure 5. a) Concentration-dependant vasorelaxation evoked by **2** (C21) and Ligand 20 in pre-contracted mouse aorta (top). b) Concentration-dependant vasorelaxation evoked by C21 in pre-contracted mouse aorta in the presence of Ligand 20 (bottom).

However, the imidazole derivative compound **3** was a somewhat less efficient inhibitor of CYP2B6 and demonstrated an IC_{50} ~20 µM to be compared to IC_{50} > 50 µM) obtained with ligand **20**. A possible explanation of the lower CYP affinities could be that the bulky *tert*-butyl group attached to the imidazole ring of ligand **20** prevents a productive coordination with the iron atom of this class of oxidative enzymes.

The apparent permeability (P_{app}) across human intestinal epithelial Caco-2 cell monolayer of the AT_2R antagonist **3** (C38) and the 20 fold more efficient AT_2R binder **20** were compared. Regarding the monolayer permeability of the ligands **3** and **19**, apical to basolateral apparent permeabilities of 3.4 x 10^{-6} cm/s and 0.4 x 10^{-6} cm/s, respectively, were observed. Furthermore, efflux ratios of 7 for compound **3** and 76 for **20** were encountered. Thus, a moderate permeability is expected for both compounds and, due to efflux, ligand **20** is predicted to be less

easi…one deduced from this *in vitro* model. These data prompted us to examine the clinical candidate **4**, which we have previously re-synthesized in our lab,[49] with an AT_2R K_i of 5.6 nM under our assay conditions, regarding both stability in microsomes and apparent permeability under experimental conditions identical to those applied herein. The stability in HLM; $t_{½}$ = 38 min, in MLM; $t_{½}$ = 90 min and in human hepatocytes $t_{½}$ = 33 min. Furthermore, an apparent permeability of 1.8 x 10^{-6} cm/s and efflux ratio of 32 were encountered. Thus, we were somewhat surprised to find that **4** (EMA401) with a relatively low apparent permeability in our *in vitro* absorption model exhibits a good oral bioavalability.[32]

Ligand **20** exhibited a) a high affinity to AT2R (K_i = 9.3 nM), b) did not significantly inhibit the CYP enzymes assessed and c) demonstrated a good stability in the human liver microsome (HLM) assay and was therefore selected for functional studies.

A brief preliminary study employing the spared nerve injury (SNI) model in mice was undertaken and aimed to assess whether ligand **20** behaves similar to the prototype AT2R antagonist PD-123319 or the AT2R antagonist **4** (EMA401), the latter extensively studied in animal models of neuropathic pain.[30–32] The results obtained suggested that ligand **20**, contrary to PD-123319 did not exert any positive impact in the SNI model (data not shown). This observation prompted us to utilize a complementary model to allow us to determine if ligand **20** might act as an agonist rather than an antagonist at the AT2 receptor.

Isolated aortic preparations from mice were previously used to determine the vascular effects of the selective AT2R agonist **2** (C21).[50] Compound C21 evoked relaxation in mouse aorta that was blocked by the nitric oxide synthase inhibitor L-NAME, suggesting that the effect of **2** (C21) was mediated by nitric oxide.[50] We report that ligand **20** presented here similarly to **2** (C21) caused a concentration-dependent vasorelaxation of pre-contracted mouse aorta (Figure 5a). In separate experiments, pre-incubation of ligand **20** at 1 and 10 µM did not inhibit **2** (C21)-induced vasorelaxation (Figure 5b).

Modelling

After independent docking explorations in GLIDE, a common binding pose was identified for the series of compounds, which in each case was refined by MD equilibration. Figure 6 depicts the proposed binding mode for the very potent compound (**20**) that is compared to binding mode of **3** (C38). A model of the binding mode of the prototype AT_2R antagonist **3** when binding to the receptor as deduced from docking redefined by molecular dynamic simulations was recently suggested.[40] The sulfonyl carbamate moiety of the high affinity ligand **20** is anchored via salt-bridge interactions with $R182^{4.64}$ and $K215^{5.42}$ and a hydrogen bond of the carbonyl with $T125^{3.33}$ (the Ballesteros-Weinstein generic amino acid numbering scheme is indicated as superscript[51]). The phenyl ring of ligand **20** is lining towards $W100^{2.60}$ and $L124^{3.32}$, allowing the *tert*-butyl imidazole substituent to accommodate within a hydrophobic cluster composed by residues $Y51^{1.39}$, $Y103^{2.64}$, $Y104^{2.65}$, $Y108^{2.69}$, $P301^{7.36}$, and $I304^{7.39}$. The side chain carbonyl group that is essential for high affinity to AT2R is bridging to $R182^{4.64}$ and $Y103^{2.64}$ via a water molecule as clearly demonstrated in Figure 6. The isobutyl group attached to the thiophene ring is placed in a deeper region of the transmembrane cavity, defined by residues $L124^{3.32}$, $M127^{3.35}$, $W269^{6.48}$, $F272^{6.51}$, and $F308^{7.43}$. Finally, the methyloxy part on the sulfonyl carbamate is located between transmembrane helices TM3-TM5 defined by the residues $Ile211^{5.38}$, $Lys215^{5.42}$, and $F129^{3.37}$. The binding mode proposed explains to a big extent the SAR for this series, as depicted in function of **20** significantly improves the affinity of the ligands as compared to **3** (C38). Furthermore, it is notable that the butoxy group of metabolically unstable compound **13** and the methyloxy group of the more stable **20** are both accommodated well in the receptor which is reflected in their similar affinities.

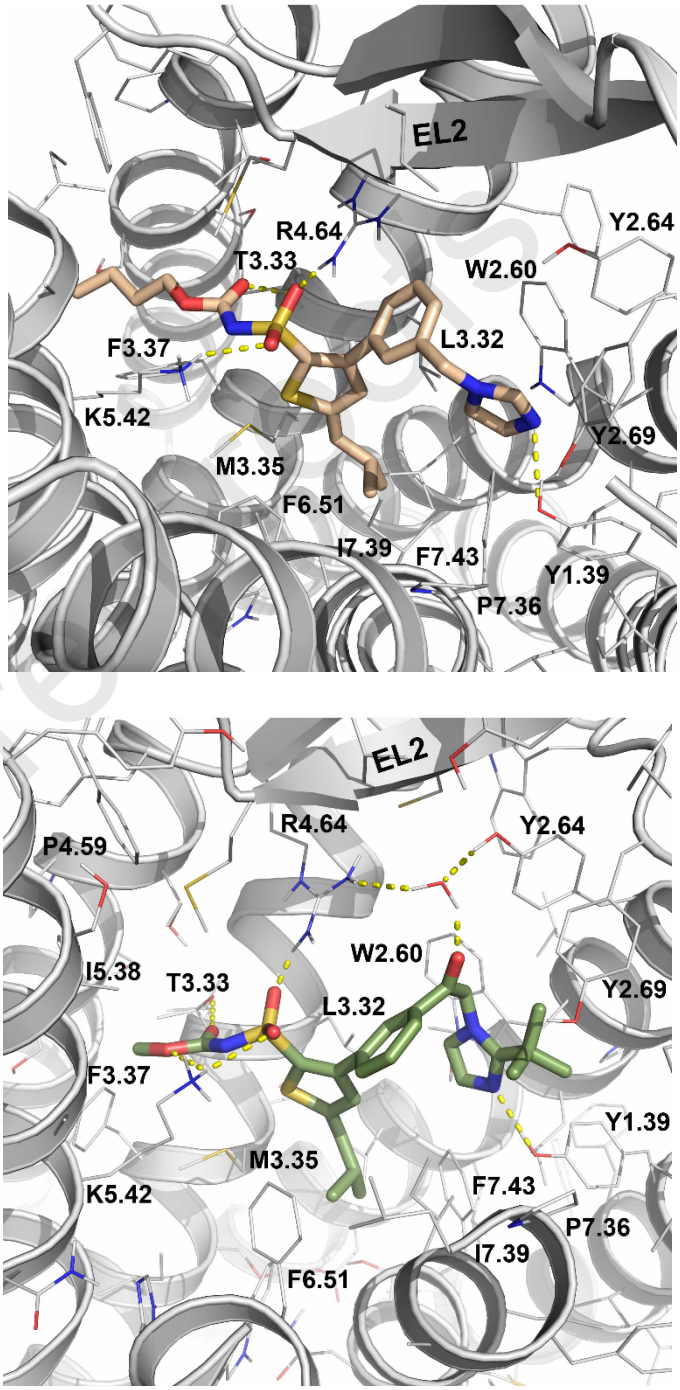

Figure 6. Compound **3** (C38) (top) and ligand **20** (bottom)

4. Conclusion

In summary, we have identified potent AT2 receptor selective ligands, among those the *tert*-butylimidazole derivative **20** (AT_2R; K_i = 9.3 nM, AT_1R; K_i > 3000 nM) that exhibits a high stability in human liver microsomes ($t_{½}$ = 62 min) and in human hepatocytes ($t_{½}$ = 194 min). Hence, this AT_2R ligand is a 20-fold more potent binder to the receptor than the selective AT_2R prototype antagonist **3** and is considerably more stable in human liver microsomes. Furthermore, it is shown that **20** is a very poor

inhi[illegible]nt at and CYP2C9 as compared to **3** (C38) that is an efficient inhibitor of these oxidative enzymes. The *tert*-butoxy derivative **20** is approximately equipotent to the former clinical candidate **4** (EMA401) regarding AT_2R affinity and exhibits a superior stability in human liver microsomes and hepatocytes but demonstrates a mediocre apparent permeability (0.4 x 10^{-6} cm/s). The P_{app} of **4** is similarly relatively moderate (1.8 x 10^{-6} cm/s) in the in vitro model applied but **4** is nevertheless absorbed from the intestine and exhibits an oral bioavailability of 33%. It is demonstrated herein that the presence of an alkoxy chain that is strongly preferred in AT_2R agonists, *e.g.* **2**, is not a requirement in this series of ligands. Docking calculations combined with molecular dynamics simulations allowed proposals of the tentative binding modes of the most potent AT_2R ligands. In functional studies, it was also shown that ligand **20** acts as an AT2R agonist and caused an AT2R mediated concentration-dependent vasorelaxation of pre-contracted mouse aorta, while it did not appear to exhibit AT2R antagonist properties, at least up to 10 μM.

5. Experimental section

5.1. Chemistry

All solvents and chemicals were used as purchased without further purification. Microwave heating was performed in a Biotage single-mode microwave reactor producing controlled irradiation at 2450 MHz with a power of 0–400 W. The reaction temperature was determined and controlled using the built-in online IR-sensor. Microwave mediated reactions were performed in septum sealed Biotage vials. Analytical TLC was performed on silica gel 60 F-254 plates and visualized with UV light (λ = 254 nm). Automated flash column chromatography was performed on Biotage Isolera or Grace Reveleris X2 instruments using commercial silica cartridges. Analytical HPLC/ESI-MS was performed using UV detection (214, 254 and 280 nm) and electrospray ionization (ESI) MS on a C18 column (50x3.0 mm, 2.6 μm particle size, 100 Å pore size) with gradients of acetonitrile in 0.05% aqueous HCOOH as mobile phase at a flow rate of 1.5 mL/min. High resolution molecular masses (HRMS) were determined on a mass spectrometer equipped with an ESI source and 7-T hybrid linear ion trap (LTQ). Nuclear magnetic resonance (NMR) spectra were recorded at 400 MHz for ^{1}H and 101 MHz for ^{13}C. Chemical shifts (δ) are reported in ppm with the residual solvent peak as internal standard (^{1}H, $CDCl_3$ at 7.26 ppm, ^{13}C, $CDCl_3$ at 77.16 ppm). Coupling constants *J* are reported in hertz (Hz). All final compounds were ≥95% pure as determined by HPLC (UV at 254 nm) and NMR.

*5.1.1. 3-(3-((1H-imidazol-1-yl)methyl)phenyl)-5-isobutylthiophene-2-carboxylic acid (**5**)*

A solution of 5-isobutyl-thiophene-2-carboxylic acid (500 mg; 2.71 mmol) in dry THF (15 mL) was cooled to -78 °C and n-BuLi (2.5 M in hexanes; 2.7 mL; 6.8 mmol) was added slowly under nitrogen. The mixture was stirred at -78 °C for 1 h before triisopropyl borate (0.94 mL; 4.1 mmol) was added slowly. The reaction mixture was stirred at room temperature overnight. The reaction was quenched with HCl (2 M; 8 mL) and extracted with EtOAc. The organic layer was dried and evaporated. The crude was dissolved in EtOH (6 mL) and $SOCl_2$ (396 μL; 5.43 mmol) was slowly added at room temperature. The mixture was heated at 70 °C overnight. The reaction mixture was then evaporated to dryness and the intermediate ethyl ester, 1-[(3-bromophenyl)methyl]imidazole (643 mg; 2.71 mmol), $Pd(dppf)Cl_2$ (99.3 mg; 0.136 mmol), K_2CO_3 (1880 mg; 13.6 [illegible] 110 °C in a sealed vial purged with nitrogen. The reaction mixture was diluted with 3 mL EtOAc and the organic layer collected, dried with $MgSO_4$, filtered and evaporated. The crude product was purified by preparative RP-HPLC (5 – 100% MeCN in water (0.05% formic acid)) to give ethyl 3-(3-((1H-imidazol-1-yl)methyl)phenyl)-5-isobutylthiophene-2-carboxylate in 44% yield (436 mg). ^{1}H NMR (400 MHz, Chloroform-*d*) δ 7.63 (s, 1H), 7.45 – 7.33 (m, 2H), 7.29 – 7.24 (m, 1H), 7.17 – 7.08 (m, 2H), 7.00 – 6.93 (m, 1H), 6.75 – 6.69 (m, 1H), 5.15 (s, 2H), 4.19 (q, J = 7.1 Hz, 2H), 2.67 (dd, J = 7.1, 0.8 Hz, 2H), 2.01 – 1.87 (m, 1H), 1.23 (t, J = 7.1 Hz, 3H), 0.98 (d, J = 6.6 Hz, 6H). ^{13}C NMR (101 MHz, Chloroform-d) δ 161.9, 150.1, 147.6, 137.3, 136.9, 135.4, 129.7, 129.4, 129.3, 128.4, 128.3, 126.7, 125.0, 119.5, 60.8, 50.9, 39.5, 30.6, 22.3, 14.2. MS (ESI): m/z calc'd for $C_{21}H_{24}N_2O_2S$: 369.1637 [M+H]+ ; found: 369.1627.

To ethyl 3-(3-((1H-imidazol-1-yl)methyl)phenyl)-5-isobutylthiophene-2-carboxylate (48.2 mg; 0.131 mmol) was added NaOH (15.7 mg; 0.392 mmol), EtOH (2 mL) and water (0.2 mL). The mixture was microwave heated at 70 °C for 1 h. The reaction mixture was neutralized with HCl (2 M) and the solvent evaporated. The residue was dissolved in acetonitrile and the mixture filtered to remove residual sodium chloride. The solvent was evaporated to give 5 in 85% yield (37.9 mg). ^{1}H NMR (400 MHz, Methanol-d4) δ 8.42 (s, 1H), 8.05 (s, 1H), 7.47 – 7.40 (m, 2H), 7.39 – 7.32 (m, 1H), 7.27 (s, 1H), 7.24 – 7.18 (m, 1H), 7.10 (s, 1H), 6.85 – 6.76 (m, 1H), 5.27 (s, 2H), 2.69 (dd, J = 7.1, 0.8 Hz, 2H), 2.00 – 1.86 (m, 1H), 0.98 (d, J = 6.6 Hz, 6H). ^{13}C NMR (101 MHz, Methanol-d4) δ 168.6, 167.2, 149.4, 146.8, 138.7, 138.1, 136.7, 130.5, 130.4, 130.2, 129.5, 127.8, 127.2, 121.6, 52.2, 40.3, 31.8, 22.6. MS (ESI): m/z calc'd for $C_{19}H_{20}N_2O_2S$: 341.1324 [M+H]+ ; found: 341.1318.

*5.1.2. 5-(3-(3-((1H-imidazol-1-yl)methyl)phenyl)-5-isobutylthiophen-2-yl)-1H-tetrazole (**6**)*

N-tert-butyl-5-isobutyl-thiophene-2-carboxamide[33] (500 mg; 2.09 mmol) was dissolved in dry THF (50 mL) and cooled to -78 °C. n-BuLi (2.5 M in hexanes; 2.1 mL; 5.2 mmol) was added slowly under a N_2 atmosphere. The mixture was stirred at -15 °C for 4 h. The solution was cooled to -78 °C and triisopropyl borate (0.725 mL; 3.14 mmol) was added slowly. The reaction mixture was stirred at room temperature overnight. The reaction was quenched with HCl (2M; 2 mL) and extracted with EtOAc. The organic layer was dried with $MgSO_4$, filtered and evaporated. To the residue was added 1-[(3-bromophenyl)methyl]imidazole (353 mg; 1.49 mmol), $Pd(dppf)Cl_2$·DCM (60.8 mg; 74.5 μmol), K_2CO_3 (1030 mg; 7.45 mmol), DME (10 mL) and water (5 mL) and the mixture was heated at 120 °C for 1 h in a sealed vial under nitrogen. The reaction mixture was diluted with 9 mL EtOAc and the organic layer dried and evaporated. The product was isolated through automated silica flash chromatography (5-10% methanol in dichloromethane) to give 3-(3-((1H-imidazol-1-yl)methyl)phenyl)-*N*-(tert-butyl)-5-isobutylthiophene-2-carboxamide in 34% yield (200 mg).

3-(3-((1H-imidazol-1-yl)methyl)phenyl)-*N*-(tert-butyl)-5-isobutylthiophene-2-carboxamide (371 mg; 0.937 mmol) was stirred in neat TFA (10 mL) at 70 °C overnight and the reaction mixture evaporated to dryness. The product was isolated through automated flash chromatography (0–7% methanol in dichloromethane) to give the primary amide in 55% yield (176 mg).

^{1}H NMR (400 MHz, Chloroform-*d*) δ 8.80 (s, 1H), 7.53 – 7.44 (m, 2H), 7.41 (s, 1H), 7.37 – 7.27 (m, 2H), 7.16 (s, 1H), 6.73 –

6.67 (m, 1H), 0.97 (d, *J* = 6.6 Hz, 6H).

To 3-(3-((1H-imidazol-1-yl)methyl)phenyl)-5-isobutylthiophene-2-carboxamide (176 mg; 0.517 mmol) in THF (3 mL) was added pyridine (0.8 mL). The mixture was stirred at room temperature for 30 min. Trifluoroacetic anhydride (87 µL; 0.62 mmol) was added at 0 °C and the reaction was stirred for 2 h at room temperature. Ice was added to the solution, which was extracted with EtOAc. The organic layer was dried with $MgSO_4$, filtered and evaporated and the residue purified by automated flash chromatography (0 – 10% MeOH in DCM) to give 3-(3-((1H-imidazol-1-yl)methyl)phenyl)-5-isobutylthiophene-2-carbonitrile in 30% yield (50 mg). ^{1}H NMR (400 MHz, Chloroform-*d*) δ 7.86 (s, 1H), 7.64 (dd, *J* = 7.9, 1.6 Hz, 1H), 7.56 – 7.41 (m, 2H), 7.25 – 7.19 (m, 1H), 7.13 (s, 1H), 6.98 – 6.88 (m, 2H), 5.20 (s, 2H), 2.72 (d, *J* = 6.9 Hz, 2H), 2.01 – 1.88 (m, 1H), 0.98 (d, *J* = 6.6 Hz, 6H).

To a 5 mL microwave vial was added 3-(3-((1H-imidazol-1-yl)methyl)phenyl)-5-isobutylthiophene-2-carbonitrile (23.7 mg; 73.7 µmol), NaN_3 (62.3 mg; 0.958 mmol), NH_4Cl (51.3 mg; 0.959 mmol) and DMF (3 mL). The vial was capped and flushed with N_2. The mixture was microwave heated at 170 °C for 15 minutes. The reaction mixture was diluted with sat. $NaHCO_3$ and washed with ethyl acetate. The aqueous layer was acidified to pH < 1 and extracted with chloroform. The organic layer was dried with $MgSO_4$, filtered and evaporated. The product was purified by preparative RP-HPLC (C8 column, 10–80% MeCN in water (0.05% formic acid). Product containing fractions were collected and the solvent evaporated to give the product in 60% yield (16.0 mg). ^{1}H NMR (400 MHz, Chloroform-*d*) δ 8.74 (s, 1H), 7.49 – 7.39 (m, 3H), 7.30 – 7.26 (m, 2H), 7.20 (s, 1H), 6.84 (s, 1H), 5.27 (s, 2H), 2.73 (d, *J* = 7.0 Hz, 2H), 2.02 – 1.89 (m, 1H), 1.01 (d, *J* = 6.6 Hz, 6H). ^{13}C NMR (126 MHz, Methanol-d_4) δ 155.3, 147.1, 141.4, 137.6, 136.2, 134.1, 130.0, 129.8, 129.7, 128.5, 127.8, 123.5, 122.1, 121.8, 52.78, 39.7, 31.2, 22.6. MS (ESI): m/z calc'd for C19H20N6S: 365.1548 [M+H]+ ; found: 365.1541.

5.1.3. Butyl ((3-(3-(2-(1H-imidazol-1-yl)acetyl)phenyl)-5-isobutylthiophen-2-yl)sulfonyl)carbamate (7)

The synthesis of **7** has been disclosed previously.[28]

5.1.4. Butyl ((5-isobutyl-3-(3-(2-(2-methyl-1H-imidazol-1-yl)acetyl)phenyl)thiophen-2-yl)sulfonyl)carbamate 2,2,2-trifluoroacetate (8)

Alkylation: A mixture of 2-bromo-1-(3-bromophenyl)ethan-1-one (111 mg, 0.400 mmol), 2-methyl-1*H*-imidazole (164 mg, 2.00 mmol) in DMF (2 mL) was heated at 100 °C overnight. The reaction mixture was evaporated and the residue purified by automated silica flash chromatography (1-10% methanol in dichloromethane). Product fractions were concentrated under reduced pressure and dried under vacuum to give 50.4 mg (45% crude) of the alkylated imidazole.

Suzuki coupling: The alkylation product (27.9 mg, 0.100 mmol), (2-(*N*-(*tert*-butyl)sulfamoyl)-5-isobutylthiophen-3-yl)boronic acid MIDA ester (51.6 mg, 0.12 mmol), K_2CO_3 (69.1 mg, 0.50 mmol), $PdCl_2$(dppf) (3.7 mg, 5.0 µmol), DME (1.0 mL) and water (0.20 mL). The vial was flushed with N_2, sealed with a screw-cap and the reaction was heated at 120 °C for 60 min. Ethyl acetate (3 mL) and water (2 mL) was added to the cooled reaction mixture and mixed thoroughly. The organic layer was separated and the aqueous layer extracted with 3 mL ethyl acetate. The combined organic layer was dried (Isolute HM-N), filtered and evaporated. The residue was carried forward to the next step.

Deprotection: To the Suzuki product was added trifluoroacetic acid (1 mL) and the mixture was stirred at 60 °C for 6 h. The reaction mixture was co-evaporated with toluene to dryness. The residue was partitioned between 3 mL dichloromethane and 2 mL sat $NaHCO_3$ (aq). The organic layer was loaded onto a plug of silica. The plug was first eluted with dichloromethane (discarded), then with 10% MeOH in dichloromethane. The product containing fraction was evaporated and used as is in the next step.

Coupling with butyl chloroformate: To a solution of the crude primary sulfonamide in dichloromethane (2 mL) was added first triethylamine (28 µL, 0.20 mmol) then butyl chloroformate (19 µL, 0.15 mmol) and the reaction mixture was stirred at room temperature overnight. The reaction mixture was diluted with 2 mL dichloromethane, washed with 1 M HCl (2 mL), dried (isolute HM-N) and loaded onto a silica plug. The plug was eluted with 10% methanol in dichloromethane the collected fraction was evaporated. The residue was purified by preparative RP-HPLC (30-60% MeCN in water [0.1% TFA]). Product fractions were freeze-dried to give 5.0 mg (8%, three step) of butyl ((5-isobutyl-3-(3-(2-(2-methyl-1*H*-imidazol-1-yl)acetyl)phenyl)thiophen-2-yl)sulfonyl)carbamate 2,2,2-trifluoroacetate. ^{1}H NMR (400 MHz, $CDCl_3$) δ 8.41 (s, 1H), 8.01 (d, *J* = 7.8 Hz, 1H), 7.67 (d, *J* = 7.7 Hz, 1H), 7.57 (t, *J* = 7.7 Hz, 1H), 7.26 – 7.21 (m, 1H), 7.19 – 7.14 (m, 1H), 6.81 (s, 1H), 5.70 (s, 2H), 4.00 (t, *J* = 6.7 Hz, 2H), 3.13 (d, *J* = 7.6 Hz, 1H), 2.73 (d, *J* = 7.1 Hz, 2H), 2.55 (s, 3H), 2.02 – 1.88 (m, 1H), 1.55 – 1.42 (m, 2H), 1.36 – 1.17 (m, 2H), 1.00 (d, *J* = 6.6 Hz, 6H), 0.86 (t, *J* = 7.4 Hz, 3H). MS (ESI): *m/z* calc'd for $C_{25}H_{32}N_3O_5S_2^+$: 518.1783 [M+H$^+$]; found: 518.1792.

5.1.5. Butyl ((3-(3-(2-(2-ethyl-1H-imidazol-1-yl)acetyl)phenyl)-5-isobutylthiophen-2-yl)sulfonyl)carbamate (9)

The synthesis of **9** has been disclosed previously.[28]

5.1.6. Butyl ((5-isobutyl-3-(3-(2-(2-propyl-1H-imidazol-1-yl)acetyl)phenyl)thiophen-2-yl)sulfonyl)carbamate (10)

Alkylation: A mixture of 2-bromo-1-(3-bromophenyl)ethan-1-one (125 mg, 0.450 mmol), 2-propyl-1*H*-imidazole (248 mg, 2.25 mmol) in DMF (2 mL) was heated at 80 °C for 2 h. The reaction mixture was evaporated and the residue purified by automated silica flash chromatography (1-7.5% methanol in dichloromethane). Product fractions were concentrated under reduced pressure and dried under vacuum to give 106 mg (77% crude) of the alkylated imidazole.

Suzuki coupling: The alkylation product (30.7 mg, 0.100 mmol), (2-(*N*-(*tert*-butyl)sulfamoyl)-5-isobutylthiophen-3-yl)boronic acid MIDA ester (51.6 mg, 0.12 mmol), K_2CO_3 (69.1 mg, 0.50 mmol), $PdCl_2$(dppf) (3.7 mg, 5.0 µmol), DME (1.0 mL) and water (0.20 mL). The vial was flushed with N_2, sealed with a screw-cap and the reaction was heated at 120 °C for 60 min. Ethyl acetate (3 mL) and water (2 mL) was added to the cooled reaction mixture and mixed thoroughly. The organic layer was separated and the aqueous layer extracted with 3 mL ethyl acetate. The combined organic layer was dried (Isolute HM-N),

filte The next step.

Deprotection: To the Suzuki product was added trifluoroacetic acid (1 mL) and the mixture was stirred at 40 °C overnight. The reaction mixture was co-evaporated with toluene to dryness. The residue was partitioned between 3 mL dichloromethane and 2 mL sat $NaHCO_3$ (aq). The organic layer was loaded onto a plug of silica. The plug was first eluted with dichloromethane (discarded), then with 10% MeOH in dichloromethane. The product containing fraction was evaporated and used as is in the next step.

Coupling with butyl chloroformate: To a solution of the crude primary sulfonamide in dichloromethane (2 mL) was added first triethylamine (28 µL, 0.20 mmol) then butyl chloroformate (19 µL, 0.15 mmol) and DMAP (1 mg) and the reaction mixture was stirred at room temperature for 1 h. The reaction mixture was diluted with 2 mL dichloromethane, washed with 1 M HCl (2 mL), dried (isolute HM-N) and evaporated. The residue was purified by silica flash chromatography (5-10% MeOH in dichloromethane). Product fractions were evaporated and dried under vacuum to give 29.2 mg (54%, three step) of butyl ((5-isobutyl-3-(3-(2-(2-propyl-1*H*-imidazol-1-yl)acetyl)phenyl)thiophen-2-yl)sulfonyl)carbamate. ^{1}H NMR (400 MHz, $CDCl_3$) δ 8.71 (s, 1H), 7.91 (d, *J* = 7.9 Hz, 1H), 7.76 (d, *J* = 7.8 Hz, 1H), 7.42 (t, *J* = 7.8 Hz, 1H), 7.08 – 7.01 (m, 2H), 6.75 (s, 1H), 5.64 (s, 2H), 3.89 (t, *J* = 6.8 Hz, 2H), 2.75 – 2.59 (m, 4H), 1.97 – 1.82 (m, 1H), 1.65 – 1.54 (m, 2H), 1.51 – 1.38 (m, 2H), 1.27 – 1.16 (m, 2H), 0.96 (d, *J* = 6.6 Hz, 6H), 0.86 – 0.78 (m, 6H). ^{13}C NMR (101 MHz, $CDCl_3$) δ 191.2, 158.6, 148.5, 147.3, 140.3, 138.9, 136.3, 134.9, 133.1, 130.9, 128.8, 128.1, 127.3, 122.2, 120.7, 65.0, 53.2, 39.3, 31.2, 30.6, 26.6, 22.4, 21.3, 19.2, 13.9, 13.6. MS (ESI): *m/z* calc'd for $C_{27}H_{36}N_3O_5S_2^+$: 546.2096 [M+H$^+$]; found: 546.2092.

5.1.7. Butyl ((5-isobutyl-3-(3-(2-(2-butyl-1H-imidazol-1-yl)acetyl)phenyl)thiophen-2-yl)sulfonyl)carbamate (11)

Alkylation: A mixture of 2-bromo-1-(3-bromophenyl)ethan-1-one (125 mg, 0.450 mmol), 2-butyl-1*H*-imidazole (279 mg, 2.25 mmol) in DMF (2 mL) was heated at 80 °C for 2 h. The reaction mixture was evaporated and the residue purified by automated silica flash chromatography (1-7.5% methanol in dichloromethane). Product fractions were concentrated under reduced pressure and dried under vacuum to give 99.3 mg (69% crude) of the alkylated imidazole.

Suzuki coupling: The alkylation product (32.1 mg, 0.100 mmol), (2-(*N*-(*tert*-butyl)sulfamoyl)-5-isobutylthiophen-3-yl)boronic acid MIDA ester (51.6 mg, 0.12 mmol), K_2CO_3 (69.1 mg, 0.50 mmol), $PdCl_2$(dppf) (3.7 mg, 5.0 µmol), DME (1.0 mL) and water (0.20 mL). The vial was flushed with N_2, sealed with a screw-cap and the reaction was heated at 120 °C for 60 min. Ethyl acetate (3 mL) and water (2 mL) was added to the cooled reaction mixture and mixed thoroughly. The organic layer was separated and the aqueous layer extracted with 3 mL ethyl acetate. The combined organic layer was dried (Isolute HM-N), filtered and evaporated. The residue was carried forward to the next step.

Deprotection: To the Suzuki product was added trifluoroacetic acid (1 mL) and the mixture was stirred at 60 °C overnight. The reaction mixture was co-evaporated with toluene to dryness. The residue was partitioned between 3 mL dichloromethane and 2 mL sat $NaHCO_3$ (aq). The organic layer was loaded onto a plug of silica. The plug was first eluted with dichloromethane (discarded), then with 10% MeOH in dichloromethane. The product containing fraction was evaporated and used as is in the next step.

Coupling with butyl chloroformate: To a solution of the crude primary sulfonamide in dichloromethane (2 mL) was added first triethylamine (17 µL, 0.12 mmol) then butyl chloroformate (13 µL, 0.10 mmol) and the reaction mixture was stirred at room temperature for 2 h. The reaction mixture was diluted with 2 mL dichloromethane, washed with 1 M HCl (2 mL), dried (isolute HM-N) and loaded onto a silica plug. The plug was eluted with 10% methanol in dichloromethane the collected fraction was evaporated. The residue was purified by preparative RP-HPLC (30-60% MeCN in water [0.05% HCOOH]). Product fractions were freeze-dried to give 5.2 mg (9%, three step) of butyl ((5-isobutyl-3-(3-(2-(2-butyl-1*H*-imidazol-1-yl)acetyl)phenyl)thiophen-2-yl)sulfonyl)carbamate. ^{1}H NMR (400 MHz, $CDCl_3$) δ 8.69 – 8.65 (m, 1H), 7.96 – 7.91 (m, 1H), 7.75 – 7.70 (m, 1H), 7.51 (t, *J* = 7.7 Hz, 1H), 7.07 – 7.01 (m, 2H), 6.79 (s, 1H), 5.55 (s, 2H), 3.95 (t, *J* = 6.8 Hz, 2H), 2.78 – 2.66 (m, 4H), 1.99 – 1.87 (m, 1H), 1.63 – 1.52 (m, 2H), 1.53 – 1.41 (m, 2H), 1.35 – 1.16 (m, 5H), 0.99 (d, *J* = 6.6 Hz, 6H), 0.89 – 0.78 (m, 6H). MS (ESI): *m/z* calc'd for $C_{28}H_{38}N_3O_5S_2^+$: 560.2253 [M+H$^+$]; found: 560.2257.

5.1.8. Butyl ((5-isobutyl-3-(3-(2-(2-isopropyl-1H-imidazol-1-yl)acetyl)phenyl)thiophen-2-yl)sulfonyl)carbamate 2,2,2-trifluoroacetate (12)

Alkylation: A mixture of 2-bromo-1-(3-bromophenyl)ethan-1-one (125 mg, 0.45 mmol), 2-isopropyl-1*H*-imidazole (248 mg, 2.25 mmol) in DMF (2 mL) was heated at 80 °C for 2 h. The reaction mixture was evaporated and the residue purified by automated silica flash chromatography (1-7.5% methanol in dichloromethane). Product fractions were concentrated under reduced pressure and dried under vacuum to give 138 mg (83% crude) of the alkylated imidazole.

Suzuki coupling: The alkylation product (30.7 mg, 0.100 mmol), (2-(*N*-(*tert*-butyl)sulfamoyl)-5-isobutylthiophen-3-yl)boronic acid MIDA ester (51.6 mg, 0.12 mmol), K_2CO_3 (69.1 mg, 0.50 mmol), $PdCl_2$(dppf) (3.7 mg, 5.0 µmol), DME (1.0 mL) and water (0.20 mL). The vial was flushed with N_2, sealed with a screw-cap and the reaction was heated at 120 °C for 60 min. Ethyl acetate (3 mL) and water (2 mL) was added to the cooled reaction mixture and mixed thoroughly. The organic layer was separated and the aqueous layer extracted with 3 mL ethyl acetate. The combined organic layer was dried (Isolute HM-N), filtered and evaporated. The residue was carried forward to the next step.

Deprotection: To the Suzuki product was added trifluoroacetic acid (3 mL) and the mixture was stirred at 60 °C for 6 h. The reaction mixture was co-evaporated with toluene to dryness. The residue was partitioned between 3 mL dichloromethane and 2 mL sat $NaHCO_3$ (aq). The organic layer was loaded onto a plug of silica. The plug was first eluted with dichloromethane (discarded), then with 10% MeOH in dichloromethane. The product containing fraction was evaporated and used as is in the next step.

Coupling with butyl chloroformate: To a solution of the crude primary sulfonamide in dichloromethane (2 mL) was added first triethylamine (28 µL, 0.20 mmol) then butyl chloroformate (19 µL, 0.15 mmol) and the reaction mixture was stirred at room temperature overnight. The reaction mixture was diluted with 2 mL dichloromethane, washed with 1 M HCl (2 mL), dried (isolute HM-N) and loaded onto a silica plug. The plug was

elute
fraction was evaporated. The residue was purified by preparative HPLC (30-60% MeCN in water [0.1% TFA]). Product fractions were freeze-dried to give 38.3 mg (58%, three step) of butyl ((5-isobutyl-3-(3-(2-(2-isopropyl-1*H*-imidazol-1-yl)acetyl)phenyl)thiophen-2-yl)sulfonyl)carbamate 2,2,2-trifluoroacetate. ^{1}H NMR (400 MHz, $CDCl_3$) δ 8.32 (s, 1H), 8.04 – 7.99 (m, 1H), 7.66 – 7.62 (m, 1H), 7.58 – 7.51 (m, 1H), 7.25 – 7.21 (s, 2H), 6.80 (s, 1H), 5.82 (s, 2H), 3.97 (t, *J* = 6.6 Hz, 2H), 3.09 2.99 (m, 1H), 2.70 (d, *J* = 7.1 Hz, 2H), 1.99 – 1.87 (m, 1H), 1.50 – 1.39 (m, 2H), 1.35 (d, *J* = 6.9 Hz, 6H), 1.26 – 1.15 (m, 2H), 0.98 (d, *J* = 6.6 Hz, 6H), 0.83 (t, *J* = 7.3 Hz, 3H). ^{13}C NMR (101 MHz, $CDCl_3$) δ 190.0, 153.2, 152.0, 151.1, 144.4, 134.9, 134.8, 133.4, 132.0, 129.5, 129.4, 129.1, 128.4, 122.6, 119.0, 66.8, 53.7, 39.4, 30.7, 30.5, 25.8, 22.3, 20.5, 18.8, 13.7. MS (ESI): *m/z* calc'd for $C_{27}H_{36}N_3O_5S_2^+$: 546.2096 [M+H$^+$]; found: 546.2099.

5.1.9. Butyl ((3-(3-(2-(2-(tert-butyl)-1H-imidazol-1-yl)acetyl)phenyl)-5-isobutylthiophen-2-yl)sulfonyl)carbamate (13)

To an 8 mL vial was added 1-(3-bromophenyl)-2-(2-(*tert*-butyl)-1*H*-imidazol-1-yl)ethan-1-one (32.1 mg, 0.100 mmol), (2-(*N*-(*tert*-butyl)sulfamoyl)-5-isobutylthiophen-3-yl)boronic acid MIDA ester (51.6 mg, 0.12 mmol), K_2CO_3 (69.1 mg, 0.5 mmol), $PdCl_2$(dppf) (3.7 mg, 5.0 µmol), DME (1 mL) and water (0.2 mL). The vial was flushed with N_2, sealed with a screw-cap and the reaction was heated at 120 °C for 60 min. Ethyl acetate (3 mL) and water (2 mL) was added to the cooled reaction mixture and mixed thoroughly. The organic layer was separated and the aqueous layer extracted with 3 mL ethyl acetate. The combined organic layer was dried (Isolute HM-N), filtered and evaporated. To the residue was added trifluoroacetic acid (1.0 mL) and the mixture was stirred at 60 °C overnight. The reaction mixture was co-evaporated with toluene to dryness and the residue was partitioned between 3 mL dichoromethane and 2 mL sat $NaHCO_3$ (aq). The organic layer was dried (Isolute HM-N), filtered loaded onto a silica plug. The silica plug was washed with dichloromethane (5 mL), then eluted with 10% methanol in dichloromethane and the collected fraction was evaporated. The residue was dissolved in dichloromethane (2 mL) and triethylamine (17µL, 0.12 mmol) was added. The mixture was cooled to 0 C and butyl chloroformate (13 µL, 0.10 mmol) was added and the mixture allowed to warm and was stirred at room temperature for 4 h. The reaction mixture was diluted with 2 mL dichloromethane, washed with 1 M HCl (2 mL), dried (isolute HM-N) and loaded onto a silica plug which was eluted with 10% methanol in dichloromethane and the collected fraction was evaporated. The residue was purified by preparative HPLC (30-60% MeCN in water [0.05% HCOOH]). Product fractions were freeze-dried to give 17.3 mg (31%, three steps) of butyl ((3-(3-(2-(2-(*tert*-butyl)-1*H*-imidazol-1-yl)acetyl)phenyl)-5-isobutylthiophen-2-yl)sulfonyl)carbamate. ^{1}H NMR (400 MHz, $CDCl_3$) δ 8.82 (s, 1H), 7.94– 7.90 (m, 1H), 7.77 – 7.70 (m, 1H), 7.49 (t, *J* = 7.8 Hz, 1H), 7.29 (s, 2H), 7.09 – 7.06 (m, 1H), 7.02 – 6.99 (m, 1H), 6.79 (s, 1H), 5.85 (s, 2H), 3.88 (t, *J* = 6.7 Hz, 2H), 2.67 (d, *J* = 7.0 Hz, 2H), 1.97 – 1.85 (m, 1H), 1.47 – 1.38 (m, 2H), 1.37 (s, 9H), 1.28 – 1.12 (m, 3H), 0.98 (d, *J* = 6.6 Hz, 6H), 0.82 (t, *J* = 7.4 Hz, 3H). ^{13}C NMR (101 MHz, $CDCl_3$) δ 191.7, 157.6, 153.3, 147.8, 140.7, 138.3, 136.0, 134.5, 133.1, 131.2, 129.0, 128.1, 127.1, 124.4, 120.8, 65.3, 55.3, 39.4, 33.8, 31.1, 30.6, 29.0, 22.5, 19.2, 13.9. MS (ESI): *m/z* calc'd for $C_{28}H_{38}N_3O_5S_2^+$: 560.2253 [M+H$^+$]; found: 560.2239.

imidazol-1-yl)acetyl)phenyl)thiophen-2-yl)sulfonyl)carbamate (14)

Alkylation: A mixture of 2-bromo-1-(3-bromophenyl)ethan-1-one (125 mg, 0.450 mmol), 2-chloro-1*H*-imidazole (46.1 mg, 0.45 mmol) and K_2CO_3 (124 mg, 0.90 mmol) in DMF (2 mL) was heated at 80 °C for 2 h. The reaction mixture was evaporated and the residue purified by automated silica flash chromatography (1-7.5% methanol in dichloromethane). Product fractions were concentrated under reduced pressure and dried under vacuum to give 87.5 mg (65% crude) of the alkylated imidazole.

Suzuki coupling: The alkylation product (30.0 mg, 0.100 mmol), (2-(*N*-(*tert*-butyl)sulfamoyl)-5-isobutylthiophen-3-yl)boronic acid MIDA ester (51.6 mg, 0.12 mmol), K_2CO_3 (69.1 mg, 0.50 mmol), $PdCl_2$(dppf) (3.7 mg, 5.0 µmol), DME (1.0 mL) and water (0.20 mL). The vial was flushed with N_2, sealed with a screw-cap and the reaction was heated at 120 °C for 60 min. Ethyl acetate (3 mL) and water (2 mL) was added to the cooled reaction mixture and mixed thoroughly. The organic layer was separated and the aqueous layer extracted with 3 mL ethyl acetate. The combined organic layer was dried (Isolute HM-N), filtered and evaporated. The residue was carried forward to the next step.

Deprotection: To the Suzuki product was added trifluoroacetic acid (1 mL) and the mixture was stirred at 60 °C overnight. The reaction mixture was co-evaporated with toluene to dryness. The residue was partitioned between 3 mL dichloromethane and 2 mL sat $NaHCO_3$ (aq). The organic layer was loaded onto a plug of silica. The plug was first eluted with dichloromethane (discarded), then with 10% MeOH in dichloromethane. The product containing fraction was evaporated and used as is in the next step.

Coupling with butyl chloroformate: To a solution of the crude primary sulfonamide in dichloromethane (2 mL) was added first triethylamine (17 µL, 0.12 mmol) then butyl chloroformate (13 µL, 0.10 mmol) and the reaction mixture was stirred at room temperature for 2 h. The reaction mixture was diluted with 2 mL dichloromethane, washed with 1 M HCl (2 mL), dried (isolute HM-N) and loaded onto a silica plug. The plug was eluted with 10% methanol in dichloromethane the collected fraction was evaporated. The residue was purified by preparative RP-HPLC (30-60% MeCN in water [0.05% HCOOH]). Product fractions were freeze-dried to give 10.3 mg (19%, three step) of butyl ((5-isobutyl-3-(3-(2-(2-chloro-1*H*-imidazol-1-yl)acetyl)phenyl)thiophen-2-yl)sulfonyl)carbamate. ^{1}H NMR (400 MHz, $CDCl_3$) δ 8.22 – 8.19 (m, 1H), 8.05 – 8.00 (m, 1H), 7.76 – 7.72 (m, 1H), 7.59 (t, *J* = 7.8 Hz, 1H), 7.03 (d, *J* = 1.5 Hz, 1H), 6.93 (d, *J* = 1.5 Hz, 1H), 6.81 (s, 1H), 5.40 (s, 2H), 4.08 (t, *J* = 6.6 Hz, 2H), 2.74 (d, *J* = 7.1 Hz, 2H), 2.05 – 1.93 (m, 1H), 1.59 – 1.47 (m, 2H), 1.35 – 1.20 (m, 2H), 1.01 (d, *J* = 6.6 Hz, 6H), 0.88 (t, *J* = 7.4 Hz, 3H). MS (ESI): *m/z* calc'd for $C_{24}H_{29}ClN_3O_5S_2^+$: 538.1237 [M+H$^+$]; found: 538.1232.

5.1.11. Butyl ((5-isobutyl-3-(3-(2-(2-bromo-1H-imidazol-1-yl)acetyl)phenyl)thiophen-2-yl)sulfonyl)carbamate (15)

Alkylation: A mixture of 2-bromo-1-(3-bromophenyl)ethane-1-one (125 mg, 0.450 mmol), 2-bromo-1*H*-imidazole (66.1 mg, 0.45 mmol) and K_2CO_3 (124 mg, 0.90 mmol) in DMF (2 mL) was heated at 80 °C for 2 h. The reaction mixture was evaporated and the residue purified by automated silica flash chromatography (1-7.5% methanol in dichloromethane). Product

frac... min. under vacuum to give 115 mg (83% crude) of the alkylated imidazole.

Suzuki coupling: The alkylation product (34.4 mg, 0.100 mmol), (2-(*N*-(*tert*-butyl)sulfamoyl)-5-isobutylthiophen-3-yl)boronic acid MIDA ester (51.6 mg, 0.12 mmol), K_2CO_3 (69.1 mg, 0.50 mmol), $PdCl_2$(dppf) (3.7 mg, 5.0 µmol), DME (1.0 mL) and water (0.20 mL). The vial was flushed with N_2, sealed with a screw-cap and the reaction was heated at 120 °C for 60 min. Ethyl acetate (3 mL) and water (2 mL) was added to the cooled reaction mixture and mixed thoroughly. The organic layer was separated and the aqueous layer extracted with 3 mL ethyl acetate. The combined organic layer was dried (Isolute HM-N), filtered and evaporated. The residue was carried forward to the next step.

Deprotection: To the Suzuki product was added trifluoroacetic acid (1 mL) and the mixture was stirred at 60 °C overnight. The reaction mixture was co-evaporated with toluene to dryness. The residue was partitioned between 3 mL dichloromethane and 2 mL sat $NaHCO_3$ (aq). The organic layer was loaded onto a plug of silica. The plug was first eluted with dichloromethane (discarded), then with 10% MeOH in dichloromethane. The product containing fraction was evaporated and used as is in the next step.

Coupling with butyl chloroformate: To a solution of the crude primary sulfonamide in dichloromethane (2 mL) was added first triethylamine (17 µL, 0.12 mmol) then butyl chloroformate (13 µL, 0.10 mmol) and the reaction mixture was stirred at room temperature for 2 h. The reaction mixture was diluted with 2 mL dichloromethane, washed with 1 M HCl (2 mL), dried (isolute HM-N) and loaded onto a silica plug. The plug was eluted with 10% methanol in dichloromethane the collected fraction was evaporated. The residue was purified by preparative RP-HPLC (30-60% MeCN in water [0.05% HCOOH]). Product fractions were freeze-dried to give 4.4 mg (8%, three step) of butyl ((5-isobutyl-3-(3-(2-(2-bromo-1*H*-imidazol-1-yl)acetyl)phenyl)thiophen-2-yl)sulfonyl)carbamate. ^{1}H NMR (400 MHz, $CDCl_3$) δ 8.22 – 8.19 (m, 1H), 8.03 (ddd, *J* = 7.8, 1.8, 1.2 Hz, 1H), 7.74 (ddd, *J* = 7.7, 1.8, 1.2 Hz, 1H), 7.59 (t, *J* = 7.7 Hz, 1H), 7.08 (d, *J* = 1.5 Hz, 1H), 7.00 (d, *J* = 1.5 Hz, 1H), 6.81 (s, 1H), 5.41 (s, 2H), 4.08 (t, *J* = 6.6 Hz, 2H), 2.74 (d, *J* = 7.1 Hz, 2H), 2.05 – 1.90 (m, 1H), 1.59 – 1.47 (m, 4H), 1.35 – 1.20 (m, 2H), 1.01 (d, *J* = 6.6 Hz, 6H), 0.88 (t, *J* = 7.4 Hz, 3H). MS (ESI): *m/z* calc'd for $C_{24}H_{29}BrN_3O_5S_2^+$: 582.0732 [M+H$^+$]; found: 582.0731.

5.1.12. Butyl ((5-isobutyl-3-(3-(2-(2-methyl-1H-benzo[d]imidazol-1-yl)acetyl)phenyl)thiophen-2-yl)sulfonyl)carbamate (16)

Alkylation: A mixture of 2-bromo-1-(3-bromophenyl)ethan-1-one (125 mg, 0.450 mmol), 2-methyl-1*H*-benzo[*d*]imidazole (59.4 mg, 0.45 mmol) and K_2CO_3 (124 mg, 0.90 mmol) in DMF (2 mL) was heated at 80 °C for 2 h. The reaction mixture was evaporated and the residue purified by automated silica flash chromatography (1-7.5% methanol in dichloromethane). Product fractions were concentrated under reduced pressure and dried under vacuum to give 80.7 mg (55% crude) of the alkylated imidazole.

Suzuki coupling: The alkylation product (32.9 mg, 0.100 mmol), (2-(*N*-(*tert*-butyl)sulfamoyl)-5-isobutylthiophen-3-yl)boronic acid MIDA ester (51.6 mg, 0.12 mmol), K_2CO_3 (69.1 mg, 0.50 mmol), $PdCl_2$(dppf) (3.7 mg, 5.0 µmol), DME (1.0 mL) and water (0.20 mL). The vial was flushed with N_2, sealed with a screw-cap and the reaction was heated at 120 °C for 60 min. Ethyl acetate (3 mL) and water (2 mL) was added to the cooled reaction mixture and mixed thoroughly. The organic layer was separated and the aqueous layer extracted with 3 mL ethyl acetate. The combined organic layer was dried (Isolute HM-N), filtered and evaporated. The residue was carried forward to the next step.

Deprotection: To the Suzuki product was added trifluoroacetic acid (1 mL) and the mixture was stirred at 40 °C overnight. The reaction mixture was co-evaporated with toluene to dryness. The residue was partitioned between 3 mL dichloromethane and 2 mL sat $NaHCO_3$ (aq). The organic layer was loaded onto a plug of silica. The plug was first eluted with dichloromethane (discarded), then with 10% MeOH in dichloromethane. The product containing fraction was evaporated and used as is in the next step.

Coupling with butyl chloroformate: To a solution of the crude primary sulfonamide in dichloromethane (2 mL) was added first triethylamine (17 µL, 0.12 mmol) then butyl chloroformate (13 µL, 0.10 mmol) and the reaction mixture was stirred at room temperature for 2 h. The reaction mixture was diluted with 2 mL dichloromethane, washed with 1 M HCl (2 mL), dried (isolute HM-N) and loaded onto a silica plug. The plug was eluted with 10% methanol in dichloromethane the collected fraction was evaporated. The residue was purified by preparative RP-HPLC (30-80% MeCN in water [0.05% HCOOH]). Product fractions were freeze-dried to give 1.6 mg (3%, three step) of butyl ((5-isobutyl-3-(3-(2-(2-methyl-1*H*-benzo[*d*]imidazol-1-yl)acetyl)phenyl)thiophen-2-yl)sulfonyl)carbamate. ^{1}H NMR (400 MHz, $CDCl_3$) δ 8.54 – 8.48 (m, 1H), 8.06 (d, *J* = 7.8 Hz, 1H), 7.92 – 7.86 (m, 1H), 7.75 (d, *J* = 7.8 Hz, 1H), 7.62 (t, *J* = 7.8 Hz, 1H), 7.50 – 7.36 (m, 3H), 6.85 (s, 1H), 5.86 (s, 2H), 4.04 (t, *J* = 6.7 Hz, 2H), 2.79 – 2.73 (m, 5H), 2.03 – 1.92 (m, 1H), 1.55 – 1.42 (m, 2H), 1.30 – 1.19 (m, 2H), 1.02 (d, *J* = 6.6 Hz, 6H), 0.85 (t, *J* = 7.4 Hz, 3H). MS (ESI): *m/z* calc'd for $C_{29}H_{34}N_3O_5S_2^+$: 568.1940 [M+H$^+$]; found: 568.1931.

5.1.13. Butyl ((5-isobutyl-3-(3-(2-(2-ethyl-1H-benzo[d]imidazol-1-yl)acetyl)phenyl)thiophen-2-yl)sulfonyl)carbamate (17)

Alkylation: A mixture of 2-bromo-1-(3-bromophenyl)ethan-1-one (125 mg, 0.450 mmol), 2-ethyl-1*H*-benzo[*d*]imidazole (65.7 mg, 0.45 mmol) and K_2CO_3 (124 mg, 0.90 mmol) in DMF (2 mL) was heated at 80 °C for 2 h. The reaction mixture was evaporated and the residue purified by automated silica flash chromatography (1-7.5% methanol in dichloromethane). Product fractions were concentrated under reduced pressure and dried under vacuum to give 73.5 mg (48% crude) of the alkylated imidazole.

Suzuki coupling: The alkylation product (34.3 mg, 0.100 mmol), (2-(*N*-(*tert*-butyl)sulfamoyl)-5-isobutylthiophen-3-yl)boronic acid MIDA ester (51.6 mg, 0.12 mmol), K_2CO_3 (69.1 mg, 0.50 mmol), $PdCl_2$(dppf) (3.7 mg, 5.0 µmol), DME (1.0 mL) and water (0.20 mL). The vial was flushed with N_2, sealed with a screw-cap and the reaction was heated at 120 °C for 60 min. Ethyl acetate (3 mL) and water (2 mL) was added to the cooled reaction mixture and mixed thoroughly. The organic layer was separated and the aqueous layer extracted with 3 mL ethyl acetate. The combined organic layer was dried (Isolute HM-N), filtered and evaporated. The residue was carried forward to the next step.

Deprotection: To the Suzuki product was added trifluoroacetic acid (1 mL) and the mixture was stirred at 40 °C overnight. The

reac ude
residue was partitioned between 3 mL dichloromethane and 2 mL sat $NaHCO_3$ (aq). The organic layer was loaded onto a plug of silica. The plug was first eluted with dichloromethane (discarded), then with 10% MeOH in dichloromethane. The product containing fraction was evaporated and used as is in the next step.

Coupling with butyl chloroformate: To a solution of the crude primary sulfonamide in dichloromethane (2 mL) was added first triethylamine (17 µL, 0.12 mmol) then butyl chloroformate (13 µL, 0.10 mmol) and the reaction mixture was stirred at room temperature. After 90 min another 5 µL butyl chloroformate was added and the reaction stirred for a further hour at room temperature. The reaction mixture was diluted with 2 mL dichloromethane, washed with 1 M HCl (2 mL), dried (isolute HM-N) and loaded onto a silica plug. The plug was eluted with 10% methanol in dichloromethane the collected fraction was evaporated. The residue was purified by preparative RP-HPLC (30-80% MeCN in water [0.05% HCOOH]). Product fractions were freeze-dried to give 1.6 mg (3%, three step) of butyl ((5-isobutyl-3-(3-(2-(2-ethyl-1*H*-benzo[*d*]imidazol-1-yl)acetyl)phenyl)thiophen-2-yl)sulfonyl)carbamate. ^{1}H NMR (400 MHz, $CDCl_3$) δ 8.36 (t, *J* = 1.7 Hz, 1H), 8.01 (dt, *J* = 7.8, 1.4 Hz, 1H), 7.79 – 7.71 (m, 2H), 7.57 (t, *J* = 7.8 Hz, 1H), 7.25 – 7.08 (m, 3H), 6.81 (s, 1H), 5.52 (s, 2H), 4.06 (t, *J* = 6.7 Hz, 2H), 2.81 – 2.68 (m, 4H), 2.03 – 1.91 (m, 1H), 1.55 – 1.36 (m, 5H), 1.29 – 1.18 (m, 2H), 1.02 (d, *J* = 6.6 Hz, 6H), 0.84 (t, *J* = 7.4 Hz, 3H). MS (ESI): *m/z* calc'd for $C_{30}H_{36}N_3O_5S_2^+$: 582.2096 [M+H$^+$]; found: 582.2104.

5.1.14. Butyl ((5-isobutyl-3-(3-(2-(2-isopropyl-1H-benzo[d]imidazol-1-yl)acetyl)phenyl)thiophen-2-yl)sulfonyl)carbamate (18)

Alkylation: A mixture of 2-bromo-1-(3-bromophenyl)ethan-1-one (125 mg, 0.450 mmol), 2-isopropyl-1*H*-benzo[*d*]imidazole (72.0 mg, 0.45 mmol) and K_2CO_3 (124 mg, 0.90 mmol) in DMF (2 mL) was heated at 80 °C for 3 h. The reaction mixture was evaporated and the residue purified by automated silica flash chromatography (1-7.5% methanol in dichloromethane). Product fractions were concentrated under reduced pressure and dried under vacuum to give 51.2 mg (32% crude) of the alkylated imidazole.

Suzuki coupling: The alkylation product (35.7 mg, 0.100 mmol), (2-(*N*-(*tert*-butyl)sulfamoyl)-5-isobutylthiophen-3-yl)boronic acid MIDA ester (51.6 mg, 0.12 mmol), K_2CO_3 (69.1 mg, 0.50 mmol), $PdCl_2$(dppf) (3.7 mg, 5.0 µmol), DME (1.0 mL) and water (0.20 mL). The vial was flushed with N_2, sealed with a screw-cap and the reaction was heated at 120 °C for 60 min. Ethyl acetate (3 mL) and water (2 mL) was added to the cooled reaction mixture and mixed thoroughly. The organic layer was separated and the aqueous layer extracted with 3 mL ethyl acetate. The combined organic layer was dried (Isolute HM-N), filtered and evaporated. The residue was carried forward to the next step.

Deprotection: To the Suzuki product was added trifluoroacetic acid (1 mL) and the mixture was stirred at 40 °C overnight. The reaction mixture was co-evaporated with toluene to dryness. The residue was partitioned between 3 mL dichloromethane and 2 mL sat $NaHCO_3$ (aq). The organic layer was loaded onto a plug of silica. The plug was first eluted with dichloromethane (discarded), then with 10% MeOH in dichloromethane. The product containing fraction was evaporated and used as is in the next step.

Coupling with butyl chloroformate: To a solution of the crude primary sulfonamide in dichloromethane (2 mL) was added first triethylamine (17 µL, 0.12 mmol) then butyl chloroformate (13 µL, 0.10 mmol) and DMAP (1 mg, cat.) and the reaction mixture was stirred at room temperature. After 90 min another 5 µL butyl chloroformate was added and the reaction stirred for a further hour at room temperature. The reaction mixture was diluted with 2 mL dichloromethane, washed with 1 M HCl (2 mL), dried (isolute HM-N) and loaded onto a silica plug. The plug was eluted with 10% methanol in dichloromethane the collected fraction was evaporated. The residue was purified by preparative RP-HPLC (30-80% MeCN in water [0.05% HCOOH]). Product fractions were freeze-dried to give 27.4 mg (46%, three step) of butyl ((5-isobutyl-3-(3-(2-(2-isopropyl-1*H*-benzo[*d*]imidazol-1-yl)acetyl)phenyl)thiophen-2-yl)sulfonyl)carbamate. ^{1}H NMR (400 MHz, $CDCl_3$) δ 8.36 – 8.32 (m, 1H), 8.05 (dt, *J* = 7.8, 1.4 Hz, 1H), 7.79 – 7.71 (m, 2H), 7.59 (t, *J* = 7.8 Hz, 1H), 7.25 – 7.08 (m, 3H), 6.81 (s, 1H), 5.58 (s, 2H), 4.05 (t, *J* = 6.6 Hz, 2H), 3.05 – 2.95 (m, 1H), 2.74 (d, *J* = 7.1 Hz, 2H), 2.04 – 1.91 (m, 1H), 1.53 – 1.37 (m, 8H), 1.28 – 1.16 (m, 2H), 1.01 (d, *J* = 6.6 Hz, 6H), 0.83 (t, *J* = 7.4 Hz, 3H). ^{13}C NMR (101 MHz, $CDCl_3$) δ 191.4, 160.3, 151.8, 151.6, 144.7, 140.5, 135.2, 134.8, 134.7, 134.1, 132.8, 129.8, 129.2, 129.1, 128.1, 123.0, 122.8, 118.7, 109.4, 66.8, 49.6, 39.5, 30.7, 30.6, 26.7, 22.4, 21.5, 18.9, 13.7. MS (ESI): *m/z* calc'd for $C_{31}H_{38}N_3O_5S_2^+$: 596.2253 [M+H$^+$]; found: 596.2254.

5.1.15. Butyl ((5-isobutyl-3-(3-(2-(5,6-dimethyl-1H-benzo[d]imidazol-1-yl)acetyl)phenyl)thiophen-2-yl)sulfonyl)carbamate (19)

Alkylation: A mixture of 2-bromo-1-(3-bromophenyl)ethan-1-one (125 mg, 0.450 mmol), 5,6-dimethyl-1*H*-benzo[*d*]imidazole (65.7 mg, 0.45 mmol) and K_2CO_3 (124 mg, 0.90 mmol) in DMF (2 mL) was heated at 80 °C for 3 h. The reaction mixture was evaporated and the residue purified by automated silica flash chromatography (1-7.5% methanol in dichloromethane). Product fractions were concentrated under reduced pressure and dried under vacuum to give 74.0 mg (48% crude) of the alkylated imidazole.

Suzuki coupling: The alkylation product (34.3 mg, 0.100 mmol), (2-(*N*-(*tert*-butyl)sulfamoyl)-5-isobutylthiophen-3-yl)boronic acid MIDA ester (51.6 mg, 0.12 mmol), K_2CO_3 (69.1 mg, 0.50 mmol), $PdCl_2$(dppf) (3.7 mg, 5.0 µmol), DME (1.0 mL) and water (0.20 mL). The vial was flushed with N_2, sealed with a screw-cap and the reaction was heated at 120 °C for 60 min. Ethyl acetate (3 mL) and water (2 mL) was added to the cooled reaction mixture and mixed thoroughly. The organic layer was separated and the aqueous layer extracted with 3 mL ethyl acetate. The combined organic layer was dried (Isolute HM-N), filtered and evaporated. The residue was carried forward to the next step.

Deprotection: To the Suzuki product was added trifluoroacetic acid (1 mL) and the mixture was stirred at 40 °C overnight. The reaction mixture was co-evaporated with toluene to dryness. The residue was partitioned between 3 mL dichloromethane and 2 mL sat $NaHCO_3$ (aq). The organic layer was loaded onto a plug of silica. The plug was first eluted with dichloromethane (discarded), then with 10% MeOH in dichloromethane. The product containing fraction was evaporated and used as is in the next step.

Coupling with butyl chloroformate: To a solution of the crude primary sulfonamide in dichloromethane (2 mL) was added first triethylamine (17 µL, 0.12 mmol) then butyl chloroformate (13

µL, temperature. After 90 min more triethylamine (17 µL, 0.12 mmol) and butyl chloroformate (13 µL, 0.10 mmol) was added and the reaction stirred for a further 90 min at room temperature. The reaction mixture was diluted with 2 mL dichloromethane, washed with 1 M HCl (2 mL), dried (isolute HM-N) and loaded onto a silica plug. The plug was eluted with 10% methanol in dichloromethane the collected fraction was evaporated. The residue was purified by preparative RP-HPLC (30-80% MeCN in water [0.05% HCOOH]). Product fractions were freeze-dried to give 5.0 mg (9%, three step) of butyl ((5-isobutyl-3-(3-(2-(5,6-dimethyl-1*H*-benzo[*d*]imidazol-1-yl)acetyl)phenyl)thiophen-2-yl)sulfonyl)carbamate. ^{1}H NMR (400 MHz, $CDCl_3$) δ 8.37 (s, 1H), 7.85 (s, 1H), 7.71 – 7.63 (m, 2H), 7.43 (t, *J* = 7.7 Hz, 1H), 7.04 (s, 1H), 6.79 (s, 1H), 5.23 (s, 2H), 4.09 (t, *J* = 6.7 Hz, 2H), 2.75 (d, *J* = 7.1 Hz, 2H), 2.34 (s, 3H), 2.30 (s, 3H), 2.02 – 1.93 (m, 1H), 1.60 – 1.51 (m, 2H), 1.33 – 1.22 (m, 2H), 1.02 (d, *J* = 6.6 Hz, 6H), 0.87 (t, *J* = 7.4 Hz, 3H). MS (ESI): *m/z* calc'd for $C_{30}H_{36}N_3O_5S_2^+$: 582.2096 [M+H$^+$]; found: 582.2090.

5.1.16. Methyl ((3-(3-(2-(2-(tert-butyl)-1H-imidazol-1-yl)acetyl)phenyl)-5-isobutylthiophen-2-yl)sulfonyl)carbamate (20)

A mixture of 2-bromo-1-(3-bromophenyl)ethane-1-one (278 mg, 1.00 mmol), 2-*tert*-butyl-1H-imidazole (149 mg, 1.2 mmol) and K_2CO_3 (276 mg, 2.0 mol) in 3 mL acetonitrile was heated at 80 °C for 2 h. The reaction mixture was evaporated and the residue purified by automated silica flash chromatography (1-7.5% methanol in dichloromethane). Product fractions were concentrated under reduced pressure and dried under vacuum to give 233 mg (73%) of 1-(3-bromophenyl)-2-(2-(*tert*-butyl)-1*H*-imidazol-1-yl)ethan-1-one.

To an 8 mL vial was added 1-(3-bromophenyl)-2-(2-(*tert*-butyl)-1*H*-imidazol-1-yl)ethan-1-one (96.4 mg, 0.300 mmol), (2-(*N*-(*tert*-butyl)sulfamoyl)-5-isobutylthiophen-3-yl)boronic acid MIDA ester (129.1 mg, 0.30 mmol), K_2CO_3 (207 mg, 1.5 mmol), $PdCl_2$(dppf) (11.0 mg, 0.015 mmol), DME (3 mL) and water (1 mL). The vial was flushed with N_2, sealed with a screw-cap and the reaction was heated at 120 °C for 60 min. Ethyl acetate (3 mL) was added to the cooled reaction mixture. The organic layer was separated and the aqueous layer extracted with 3 mL ethyl acetate. The combined organic layer was dried (Isolute HM-N), filtered and evaporated and purified by automated flash chromatography (2.5-7.5% MeOH in dichloromethane). Product fractions were concentrated under reduced pressure and dried under vacuum.

To the residue was added trifluoroacetic acid (4 mL) and the mixture was stirred at room temperature over the weekend, then heated at 60 °C for 5 h. The reaction mixture was co-evaporated with toluene to dryness and the residue was partitioned between 5 mL ethyl acetate and 5 mL sat $NaHCO_3$ (aq). The organic layer was dried (Isolute HM-N), filtered and evaporated.

A solution of the crude primary sulfonamide in dichloromethane (3 mL) was treated with first DIEA (0.16 mL, 0.91 mmol) and DMAP (2 mg, cat) then methyl chloroformate (23µL, 0.30 mmol) and the reaction mixture was stirred at room temperature overnight (15 h). The reaction mixture was washed with sat. NH4Cl (aq) (3 mL) and brine (3 mL). The organic layer was dried (Isolute HM-N), filtered and evaporated and the residue purified by automated silica flash chromatography (2.5-10% methanol in dichloromethane). Product fractions were concentrated under reduced pressure and dried under vacuum to give 61.2 mg (39%, three step) of methyl ((3-(3-(2-(2-(*tert*-yl)sulfonyl)carbamate. ^{1}H NMR (400 MHz, $CDCl_3$) δ 8.90 (s, 1H), 7.92 – 7.87 (m, 1H), 7.77 – 7.72 (m, 1H), 7.46 (t, *J* = 7.8 Hz, 1H), 7.13 – 7.07 (m, 2H), 6.77 (s, 1H), 5.91 (s, 2H), 3.43 (s, 3H), 2.64 (d, *J* = 7.0 Hz, 2H), 1.97 – 1.83 (m, 1H), 1.36 (s, 9H), 0.96 (d, *J* = 6.6 Hz, 6H). ^{13}C NMR (101 MHz, $CDCl_3$) δ 191.7, 159.3, 153.0, 147.2, 140.1, 138.8, 136.1, 134.7, 132.8, 131.3, 128.9, 128.0, 127.1, 124.8, 119.7, 55.6, 52.3, 39.3, 33.8, 30.6, 28.8, 22.4. MS (ESI): *m/z* calc'd for $C_{25}H_{32}N_3O_5S_2^+$: 518.1783 [M+H$^+$]; found: 518.1796.

5.1.17. Methyl ((3-(3-(2-(2-cyclopropyl-1H-imidazol-1-yl)acetyl)phenyl)-5-isobutylthiophen-2-yl)sulfonyl)carbamate (21)

To a solution of 3-(3-(2-(2-cyclopropyl-1H-imidazol-1-yl)acetyl)phenyl)-5-isobutylthiophene-2-sulfonamide (16.0 mg, 0.036 mmol) in dichloromethane (2 mL) was added first DIEA (25 µL, 0.14 mmol) then methyl chloroformate (3.3 µL, 0.043 mmol) and the reaction mixture was stirred at room temperature for 90 min. The reaction mixture was then evaporated and the residue purified by automated silica flash chromatography (5-20% methanol in dichloromethane). Product fractions were concentrated under reduced pressure and dried under vacuum to give 10.2 mg (56%) of methyl ((3-(3-(2-(2-cyclopropyl-1*H*-imidazol-1-yl)acetyl)phenyl)-5-isobutylthiophen-2-yl)sulfonyl)carbamate. ^{1}H NMR (400 MHz, $CDCl_3$) δ 8.52 – 8.49 (m, 1H), 8.02 (d, *J* = 7.8 Hz, 1H), 7.69 (d, *J* = 7.7 Hz, 1H), 7.58 (t, *J* = 7.7 Hz, 1H), 7.23 – 7.15 (m, 2H), 6.82 (d, *J* = 0.8 Hz, 1H), 5.84 (s, 2H), 3.59 (s, 3H), 2.72 (d, *J* = 6.9 Hz, 2H), 2.03 – 1.79 (m, 2H), 1.26 – 1.09 (m, 4H), 1.00 (d, *J* = 6.6 Hz, 6H). MS (ESI): *m/z* calc'd for $C_{24}H_{28}N_3O_5S_2^+$: 502.1470 [M+H$^+$]; found: 502.1488.

5.1.18. Ethyl ((3-(3-(2-(2-cyclopropyl-1H-imidazol-1-yl)acetyl)phenyl)-5-isobutylthiophen-2-yl)sulfonyl)carbamate (22)

Alkylation: A mixture of 2-bromo-1-(3-bromophenyl)ethan-1-one (69.5 mg, 0.25 mmol), 2-cyclopropyl-1*H*-imidazole (81.1 mg, 0.75 mmol), K_2CO_3 (69.1 mg, 0.50 mmol) in 2 mL DMF was heated at 80 °C for 1 h. The reaction mixture was evaporated and the residue purified by automated silica flash chromatography (2-10% methanol in dichloromethane). Product fractions were concentrated under reduced pressure and dried under vacuum to give 64.9 mg (85% crude) of the alkylated imidazole.

Suzuki coupling: The intermediate (64.9 mg, 0.21 mmol), (2-(*N*-(*tert*-butyl)sulfamoyl)-5-isobutylthiophen-3-yl)boronic acid MIDA ester (91.5 mg, 0.21 mmol), K_2CO_3 (147 mg, 1.1 mmol), $PdCl_2$(dppf) (7. 8 mg, 0.011 mmol), DME (3 mL) and water (1 mL). The vial was flushed with N_2, sealed with a screw-cap and the reaction was heated at 120 °C for 60 min.[61] The organic layer was evaporated and purified by automated flash chromatography (5-15% MeOH in dichloromethane). Product fractions were concentrated under reduced pressure and dried under vacuum to give 92.3 mg (87% crude) of the Suzuki product.

Deprotection: To the Suzuki product was added trifluoroacetic acid (3 mL) and the mixture was stirred at 60 °C for 2 h. The reaction mixture was co-evaporated with toluene to dryness. The residue was partitioned between 10 mL EtOAc and 10 mL sat $NaHCO_3$ (aq). The organic layer was dried (Isolute HM-N), filtered, evaporated and dried under vacuum to give 64.5 mg (79%) of the primary sulfonamide.

primary sulfonamide (32.0 mg, 0.072 mmol) in dichloromethane (2 mL) was added first DIEA (50 µL, 0.29 mmol) then Ethyl chloroformate (8.3 µL, 0.086 mmol) and the reaction mixture was stirred at room temperature for 1 h whereby product and double acylation (m/z 588 = product + one extra ethyl carbamate) was detected. Added 200 µL ethanol and heated at 60 °C for 2 h in order to cleave off the extra carbamate. The reaction mixture was then evaporated and the residue purified by automated silica flash chromatography (5-15% methanol in dichloromethane). Product fractions were concentrated under reduced pressure and dried under vacuum to give 18.3 mg (49% crude) of ethyl ((3-(3-(2-(2-cyclopropyl-1*H*-imidazol-1-yl)acetyl)phenyl)-5-isobutylthiophen-2-yl)sulfonyl)carbamate. ^{1}H NMR (400 MHz, $CDCl_3$) δ 8.68 (s, 1H), 7.95 – 7.89 (m, 1H), 7.78 – 7.73 (m, 1H), 7.49 – 7.41 (m, 1H), 7.05 (s, 1H), 6.96 (s, 1H), 6.76 (s, 1H), 5.71 (s, 2H), 3.93 (q, *J* = 7.1 Hz, 2H), 2.65 (d, *J* = 7.2 Hz, 2H), 1.98 – 1.83 (m, 1H), 1.81 – 1.69 (m, 1H), 1.10 – 0.91 (m, 13H). ^{13}C NMR (101 MHz, $CDCl_3$) δ 191.3, 157.7, 149.3, 147.9, 140.8, 138.0, 136.1, 134.8, 133.4, 130.7, 128.9, 128.3, 127.4, 122.3, 120.7, 61.3, 53.2, 39.3, 30.6, 22.4, 14.6, 7.7, 6.0. MS (ESI): *m/z* calc'd for $C_{25}H_{30}N_3O_5S_2^+$: 516.1627 [M+H$^+$]; found: 516.1623.

5.1.19. Ethyl ((3-(3-(2-(2-(tert-butyl)-1H-imidazol-1-yl)acetyl)phenyl)-5-isobutylthiophen-2-yl)sulfonyl)carbamate (23)

A solution of butyl ((3-(3-(2-(2-(*tert*-butyl)-1*H*-imidazol-1-yl)acetyl)phenyl)-5-isobutylthiophen-2-yl)sulfonyl)carbamate (**13**) (10.0 mg, 0.0179 mmol) in ethanol (0.7 mL) was heated at 100 °C for 30 min. The reaction mixture was evaporated and the residue purified by automated silica flash chromatography (5-10% methanol in dichloromethane. Product fractions were concentrated under reduced pressure and dried under vacuum overnight to give 4.7 mg (49%) of ethyl ((3-(3-(2-(2-(*tert*-butyl)-1*H*-imidazol-1-yl)acetyl)phenyl)-5-isobutylthiophen-2-yl)sulfonyl)carbamate. ^{1}H NMR (400 MHz, $CDCl_3$) δ 8.72 (s, 1H), 7.97 (d, *J* = 7.8, 1H), 7.73 (d, *J* = 7.8 Hz, 1H), 7.54 (t, *J* = 7.8 Hz, 1H), 7.15-7.08 (m, 2H), 6.81 (s, 1H), 5.87 (s, 2H), 3.98 (q, *J* = 7.1 Hz, 2H), 2.70 (d, *J* = 7.0 Hz, 2H), 2.00 – 1.87 (m, 1H), 1.40 (s, 9H), 1.10 (t, *J* = 7.1 Hz, 3H), 1.00 (d, *J* = 6.6 Hz, 6H). ^{13}C NMR (101 MHz, $CDCl_3$) δ 191.5, 155.1, 153.3, 149.4, 142.1, 136.1, 135.7, 134.6, 133.3, 130.8, 129.2, 128.4, 127.5, 124.4, 120.9, 61.9, 55.2, 39.4, 33.8, 30.7, 29.2, 22.4, 14.5. MS (ESI): *m/z* calc'd for $C_{26}H_{34}N_3O_5S_2^+$: 532.1940 [M+H$^+$]; found: 532.1932.

5.1.20. N-((3-(3-(2-(2-(tert-butyl)-1H-imidazol-1-yl)acetyl)phenyl)-5-isobutylthiophen-2-yl)sulfonyl)acetamide (24)

To a solution of 3-(3-(2-(2-(*tert*-butyl)-1H-imidazol-1-yl)acetyl)phenyl)-5-isobutylthiophene-2-sulfonamide (16.5 mg, 0.0359 mmol) in dichloromethane (1 mL) was added first DIEA (25 µL, 0.14 mmol) then acetyl chloride (3.1 µL, 0.043 mmol) and the reaction mixture was stirred at room temperature for 90 min. The reaction mixture was washed with sat NH_4Cl (aq) (3 mL) and brine (3 mL). The organic layer was dried (Isolute HM-N), filtered and evaporated and the residue purified by automated silica flash chromatography (5-10% methanol in dichloromethane). Product fractions were concentrated under reduced pressure and dried under vacuum to give 10.2 mg. (57%) of *N*-((3-(3-(2-(2-(*tert*-butyl)-1*H*-imidazol-1-yl)acetyl)phenyl)-5-isobutylthiophen-2-yl)sulfonyl)acetamide. ^{1}H NMR (400 MHz, $CDCl_3$) δ 8.59 (s, 1H), 7.98 – 7.91 (m, 1H), 7.75 – 7.69 (m, 1H), 7.57 – 7.48 (m, 1H), 7.00 – 6.94 (m, 2H), 6.78 (s, 1H), 5.75 (s, 2H), 1.35 (s, 9H), 0.98 (d, *J* = 7.0 Hz, 6H). ^{13}C NMR (101 MHz, $CDCl_3$) δ 192.0, 173.8, 153.7, 149.4, 142.3, 135.7, 134.5, 133.6, 130.4, 129.1, 128.5, 127.6, 124.2, 122.6, 54.7, 39.4, 33.7, 30.7, 29.4, 24.8, 22.4. MS (ESI): *m/z* calc'd for $C_{25}H_{32}N_3O_4S_2^+$: 502.1834 [M+H$^+$]; found: 502.1840.

5.2. Stability in liver microsomes

Human and mouse liver microsomes obtained from XenoTech LLC, KS, USA were used to determine the metabolic stability. Metabolic stability was determined in 0.5 mg/mL human or mouse liver microsomes at a compound concentration of 1 µM in 100 mM potassium phosphate buffer (pH 7.4) in a total incubation volume of 500 µL. The reaction was initiated by addition of 1 mM NADPH. At various incubation times, i.e. at 0, 5, 10, 20, 40 and 60 min, a sample was withdrawn from the incubation and the reaction was terminated by addition of ice-cold acetonitrile containing Warfarin as internal standard. The amount of parent compound remaining was analysed by LC-MS/MS. The LC-MS/MS system used was an Acquity UPLC coupled to a triple quadrupole mass spectrometer (Waters), operating in multiple reaction monitoring (MRM) mode with positive or negative electrospray ionization. Mass spectrometric settings were optimized for each compound for one MRM transition. Chromatographic separation was typically done on a C18 Ethylene Bridged Hybrid (BEH) 1.7 µm column using a general gradient of 1% to 90% of mobile phase consisting of A, 5% acetonitrile and 0.1% formic acid in purified water, and B, 0.1% formic acid in 100% acetonitrile, over a total running time of 2 min. In a few cases, separation was done on a HSS T3 2x50 mm 2.1 µm column using a mobile phase consisting of A, 0.05% heptafluorobutyric acid (HFBA) and 0.05% propionic acid (PA) in water, and B, 0.05% HFBA and 0.05% PA in acetonitrile, with a total running time of 2 min. In both cases, the flow rate was set to 0.5 mL/min and 5 µL of the sample was injected. *In vitro* half-life ($t_{½}$) and in vitro intrinsic clearance (Cl_{int}) were calculated using previously published models.[52,53]

5.3. Metabolic stability in human hepatocytes

Metabolic stability assay was performed in cryopreserved hepatocytes from one healthy donor.[54] A simple approach for restoration of differentiation and function in cryopreserved human hepatocytes.) Thawed hepatocytes were resuspended in pre-warmed Williams medium E. The incubation was carried out on a heater-shaker at 37°C, using about 350 000 cells/ml and a final compound concentration of 1 µM. Samples were withdrawn at different time-points and the reaction was quenched by adding ice-cold acetonitrile containing 50 nM Warfarin as internal control. Samples were centrifuged at 3000 rpm for 15 min and before analysis of parent compound remaining by LC-MS/MS as described above.

5.4. CYP inhibition assay

The activity of human cytochrome P450 (CYP) was determined in human liver microsomes by following the formation of a metabolite of the probe substrate. Substrates and their concentrations for the incubation were: CYP2B6, Bupropion (80 µM); CYP2C9, Diclofenac (5 µM); CYP2D6 Bufuralol (2 µM); CYP3A4, Midazolam (2µM). The incubations contained 0.1 mg/ml human liver microsomes in 0.1 M phosphate buffer (pH 7.4) and 1 mM NDAPH. The potency of compound on the CYP enzymes was tested at concentrations

betv ctile
inhibitors were dissolved in DMSO, while substrate compounds were dissolved in acetonitrile or methanol. The final solvent concentration in all incubations was below 0.5%. In reversible inhibition incubations, inhibitor or buffer control and substrate were premixed with microsomes and buffer for 3 min before addition of 1.0 mM NADPH, which initiated the reactions. The final incubations were performed in at 37°C in a shaking incubator block. Reactions were terminated by adding icecold acetonitrile containing 100 nM warfarin as internal standard to the incubations. Samples were thereafter placed on ice for at least 15 min before centrifugation at 3500 rpm, 4 °C for 20 min. The supernatants were collected and analysed by LC-MS/MS as described above.

5.5. Caco-2 cell permeability assay

Permeability measurements were performed as previously described.[55] Caco-2 cell monolayers (passage 94-105) were grown on permeable filter supports and used for transport studies on day 21 after seeding. Prior to start of the experiment, culture medium was replaced with preheated Hank's Balanced Salt Solution (HBSS) buffered with HEPES to pH 7.4. Apparent permeability was measured, at a compound concentration of 5 µM, in both apical-to-basolateral (A-B) and basolateral-to-apical (B-A) direction at pH 7.4 using a shaking speed of 500 rpm. Immediately after the start of the experiment, a sample was removed from the donor compartment (C0), and subsequent samples were taken from the receiver compartment at 15, 30 and 60 min. At the end of the experiment (t=60 min), a sample was removed from the donor chamber (Cf) for mass balance calculation. Each experimental condition was assayed in triplicate. Compound concentration was determined by LC-MS/MS as described above.

5.6. Radioligand binding assays

All synthesized ligands were evaluated in a radioligand binding assay performed by Eurofins Cerep SA, France, by displacing [^{125}I][Sar^{1}Ile^{8}]-angiotensin II from HEK-293 cells expressing human AT_2R. [Sar^{1}Ile^{8}]-angiotensin II (Sarile) acts as a nonselective AT_2R agonist.[47] The affinity was determined using a seven-point dose-response curve and the measurements were performed in duplicates, the AT_2R selective antagonist PD-123,319 was used as reference compound. The compounds were also evaluated for inhibition of [^{125}I][Sar^{1}Ile^{8}]-angiotensin II binding to human AT_1R expressed in HEK-293 cells. For AT_1R the percent inhibition was determined at 10 µM, in duplicates, with the endogenous ligand (angiotensin II) used as reference.

5.7. Vasorelaxation

Male FVB/N mice (approximately 10-12 weeks old) were humanely killed by isoflurane inhalation and the thoracic aorta was cut into 2-3 mm lengths and mounted for isometric force recording in myographs (model 610M; DMT, Australia) connected to a Powerlab 8/35 channel recorder (ADInstruments, Australia). Vessels were maintained in physiological salt solution comprising (in mM) NaCl 118, KCl 4.7, $KH_2 \cdot PO_4$ 1.2, $MgSO_4 \cdot 7H_2O$ 1.2, $CaCl_2$ 2.5, $NaHCO_3$ 25 and glucose 11.7) at 37 °C with carbogen (95% O_2 and 5% CO_2). The tension of the vessels was gradually stretched to 0.5 g resting tension over approximately 30 minutes. After an additional 15 min equilibration at 0.5 g, the thromboxane A2 receptor agonist response. When the response plateaued, tissues were washed with Krebs solution a number of times until the tissue returned to baseline. Tissues were then pre-contracted to 30-40% maximal contraction of U44619, after which a concentration response curve was performed to the vasorelaxant effects of either **2** (C21) or ligand **20** in parallel experiments. A time control was also obtained whereby a vessel was precontracted by U46619 for the duration of the time taken to perform concentration response curves. In separate experiments, ligand **20** was also tested as a potential AT2R antagonist against **2** (C21). To this end, tissues were pre-incubated with **20** for 30 min prior to U46619-induced contraction and subsequent concentration response curves to **2** (C21).

5.8. Computational methods

5.8.1. Modelling experiments

The crystal structure of the active-like human AT2R was retrieved from the Protein Data Bank (PDB code 5UNG with antagonist L-161,638.[56,57] and was subject to preparation and minor modifications with the Schrödinger suite (Schrödinger Release 2017-3, Schrödinger, LSS, New York, NY, 2017), including (i) deletion of the engineered B562RIL protein (fused to the truncated N-terminus); (ii) addition of protons, assessment of the rotamers for Asn/Gln/His residues, and protonated state for titratable residues, resulting in all Asp, Gln, Lys, and Arg residues assigned to their default charged state and all His modelled as neutral with the proton on Nδ; (iii) addition of missing side chains, modelling the most probable conformer based on additional crystal structures of AT2 and the related AT1 receptor.

5.8.2. Ligand docking

Ligands from Figure 2 and 4 were built and their 3D conformation were optimized using the Maestro graphical interface and the LigPrep utility from the Schrödinger suite (Schrödinger Release 2017-3: Maestro, Schrödinger, LSS, New York, NY, 2017; Schrödinger Release 2017-3: LigPrep, Schrödinger, LSS, New York, NY, 2017). This method also allowed determination of their most probable protonation state at physiological pH, with a net negative change localized on the sulfonylcarbamate group in all cases. Docking was performed with Glide SP using default settings (Schrödinger Release 2017-3: Glide, Schrödinger, LSS, New York, NY, 2017).[58–60] The docking grid centroid was placed taken as reference the coordinates of the co-crystallized ligand L-161,638, and expanding the cubic grid box was set to 30 Å on each dimensions. The selection of poses was done on the basis of a double criterion, combining the highest possible scoring while looking for the consensus among all ligands in the series.

5.8.3. Membrane insertion and Molecular Dynamics equilibration

Each Ligand receptor complex obtained in the previous stage was subject to an MD equilibration following the PyMedDyn protocol, as implemented in a GPCR-ModSim web server.[62,63] Briefly, the receptor-ligand complex was inserted in a pre-equilibrated membrane consisting of 1-palmitoyl-2-oleoyl phosphatidylcholine (POPC) lipids, with the transmembrane (TM) bundle aligned to its vertical axis. The simulation box was created with a hexagonal-prism geometry, which was soaked with bulk water and energy-minimized using the OPLS-AA force field for proteins and ligands, combined with the Berger parameters for the lipids.[62,64–66] It follows a molecular dynamics

equi
NPT ensemble with the GROMACS simulation package.[64]

The first phase consists of 2.5 ns with a gradual release of harmonic restraints on protein (and ligand) heavy atoms. The second phase consists of free MD for another 2.5 ns, except for weak distance restraints between 24 pairs of interacting residues corresponding to conserved positions within the TM bundle of class-A GPCRs with a structural role.[63,67] The final snapshot was energy minimized and retained for analysis and figures.

Acknowledgments

We thank the Kjell and Märta Beijer Foundation and the Swedish Brain Foundation for financial support, the SciLifeLab Drug Discovery and Development Platform for support with compound syntheses and ADME evaluations and the Swedish National Infrastructure for Computing (SNIC) for computational resources. This work was supported in part by the National Health and Medical Research Council (NHMRC) of Australia (GNT1127792) to REW. Centre for Preclinical Research and Technology, Medical University of Warsaw infrastructure was used in the conduction of the study.

Appendix A. Supplementary material

Supplementary data to this article can be found online at https://doi.

References and notes

1. Ondetti MA, Rubin B, Cushman DW. Design of specific inhibitors of angiotensin-converting enzyme: new class of orally active antihypertensive agents. *Science (80-)*. 1977;196(4288):441-444. doi:10.1126/science.191908
2. Ondetti MA, Cushman DW. Inhibition of the renin-angiotensin system. A new approach to the therapy of hypertension. *J Med Chem*. 1981;24(4):355-361. doi:10.1021/jm00136a001
3. Azizi M, Webb R, Nussberger J, Hollenberg NK. Renin inhibition with aliskiren: where are we now, and where are we going? *J Hypertens*. 2006;24(2):243-256. doi:10.1097/01.hjh.0000202812.72341.99
4. Wexler RR, Greenlee WJ, Irvin JD, et al. Nonpeptide Angiotensin II Receptor Antagonists: The Next Generation in Antihypertensive Therapy. *J Med Chem*. 1996;39(3):625-656. doi:10.1021/jm9504722
5. Paulis L, Steckelings UM, Unger T. Key advances in antihypertensive treatment. *Nat Rev Cardiol*. 2012;9(5):276-285. doi:10.1038/nrcardio.2012.33
6. Hallberg M. Neuropeptides: Metabolism to Bioactive Fragments and the Pharmacology of Their Receptors. *Med Res Rev*. 2015;35(3):464-519. doi:10.1002/med.21323
7. Paulis L, Unger T. Novel therapeutic targets for hypertension. *Nat Rev Cardiol*. 2010;7(8):431-441. doi:10.1038/nrcardio.2010.85
8. Gallo-Payet N, Shum M, Baillargeon J-P, et al. AT2 Receptor Agonists: Exploiting the Beneficial Arm of Ang II Signaling. *Curr Hypertens Rev*. 2012;8(1):47-59. doi:10.2174/157340212800504990
9. Juillerat-Jeanneret L. The Other Angiotensin II Receptor: AT 2 R as a Therapeutic Target. *J Med Chem*. 2020;63(5):1978-1995. doi:10.1021/acs.jmedchem.9b01780
10. Bennion DM, Steckelings UM, Sumners C. Neuroprotection via AT2 receptor agonists in ischemic stroke. *Clin Sci*. 2018;132(10):1055-1067. doi:10.1042/CS20171549
11. Wang Y, Del Borgo M, Lee HW, et al. Anti-fibrotic Potential of AT2 Receptor Agonists. *Front Pharmacol*. 2017;8(AUG):1-7. doi:10.3389/fphar.2017.00564
12. Steckelings UM, Rompe F, Kaschina E, et al. The past, present and future of angiotensin II type 2 receptor stimulation. *J Renin-Angiotensin-Aldosterone Syst*. 2010;11(1):67-73. doi:10.1177/1470320309347791
13. Sumners C, de Kloet AD, Krause EG, Unger T, Steckelings UM. Angiotensin type 2 receptors: blood pressure regulation and end organ damage. *Curr Opin Pharmacol*. 2015;21:115-121.
14. Carey RM. Angiotensin type-2 receptors and cardiovascular function: are angiotensin type-2 receptors protective? *Curr Opin Cardiol*. 2005;20(4):264-269. doi:10.1097/01.hco.0000166596.44711.b4
15. Gallinat S, Yu M, Dorst A, Unger T, Herdegen T. Sciatic nerve transection evokes lasting up-regulation of angiotensin AT2 and AT1 receptor mRNA in adult rat dorsal root ganglia and sciatic nerves. *Mol Brain Res*. 1998;57(1):111-122. doi:10.1016/S0169-328X(98)00079-5
16. Nakajima M, Hutchinson HG, Fujinaga M, et al. The angiotensin II type 2 (AT2) receptor antagonizes the growth effects of the AT1 receptor: gain-of-function study using gene transfer. *Proc Natl Acad Sci*. 1995;92(23):10663-10667. doi:10.1073/pnas.92.23.10663
17. Altarche-Xifró W, Curato C, Kaschina E, et al. Cardiac c-kit+AT2+ Cell Population is Increased in Response to Ischemic Injury and Supports Cardiomyocyte Performance. *Stem Cells*. 2009;27(10):2488-2497. doi:10.1002/stem.171
18. Busche S, Gallinat S, Bohle R-M, et al. Expression of Angiotensin AT1 and AT2 Receptors in Adult Rat Cardiomyocytes after Myocardial Infarction. *Am J Pathol*. 2000;157(2):605-611. doi:10.1016/S0002-9440(10)64571-3
19. Nio Y, Matsubara H, Murasawa S, Kanasaki M, Inada M. Regulation of gene transcription of angiotensin II receptor subtypes in myocardial infarction. *J Clin Invest*. 1995;95(1):46-54. doi:10.1172/JCI117675
20. Li J, Culman J, Hörtnagl H, et al. Angiotensin AT2 receptor protects against cerebral ischemia-induced neuronal injury. *FASEB J*. 2005;19(6):617-619. doi:10.1096/fj.04-2960fje
21. Horiuchi M, Mogi M, Iwai M. The angiotensin II type 2 receptor in the brain. *J Renin-Angiotensin-Aldosterone Syst*. 2010;11(1):1-6. doi:10.1177/1470320309347793
22. de Gasparo M, Catt KJ, Inagami T, Wright JW, Unger T. International union of pharmacology. XXIII. The angiotensin II receptors. *Pharmacol Rev*. 2000;52(3):415-472. doi:34/848966
23. Carey RM, Wang ZQ, Siragy HM. Role of the angiotensin type 2 receptor in the regulation of blood pressure and renal function. *Hypertension*. 2000;35(1 Pt 2):155-163. doi:10.1161/01.HYP.35.1.155
24. Larhed M, Hallberg M, Hallberg A. Nonpeptide AT2 Receptor Agonists. *Med Chem Rev*. 2016;51:69-82.
25. Hallberg M, Sumners C, Steckelings UM, Hallberg A. Small-molecule AT2 receptor agonists. *Med Res Rev*. 2018;38:602-624. doi:10.1002/med.21449
26. Hallberg A, Sävmarker J, Hallberg M. Angiotensin Peptides as AT2 Receptor Agonists. *Curr Protein Pept Sci*. 2017;18(8):809-818. doi:10.2174/1389203718666170203150344
27. Wan Y, Wallinder C, Plouffe B, et al. Design, synthesis, and biological evaluation of the first selective nonpeptide AT2 receptor agonist. *J Med Chem*. 2004;47(24):5995-6008. doi:10.1021/jm049715t
28. Murugaiah a MS, Wu X, Wallinder C, et al. From the first selective non-peptide AT(2) receptor agonist to structurally related antagonists. *J Med Chem*. 2012;55(5):2265-2278. doi:10.1021/jm2015099
29. Rice A, Smith M. Angiotensin II Type 2-Receptor: New Clinically Validated Target in the Treatment of Neuropathic Pain. *Clin Pharmacol Ther*. 2015;97(2):128-130. doi:10.1002/cpt.29
30. Rice ASC, Dworkin RH, McCarthy TD, et al. EMA401, an orally administered highly selective angiotensin II type 2 receptor antagonist, as a novel treatment for postherpetic neuralgia: a randomised, double-blind, placebo-controlled phase 2 clinical trial. *Lancet*. 2014;383(9929):1637-1647. doi:10.1016/S0140-6736(13)62337-5
31. Smith MT, Anand P, Rice ASC. Selective small molecule angiotensin II type 2 receptor antagonists for neuropathic pain. *Pain*. 2016;157:S33-S41. doi:10.1097/j.pain.0000000000000369
32. Keppel Hesselink J, Schatman ME. EMA401: an old antagonist of the AT2R for a new indication in neuropathic pain. *J Pain Res*. 2017;Volume 10:439-443. doi:10.2147/JPR.S128520
33. Wu X, Wan Y, Mahalingam a K, et al. Selective angiotensin II AT2 receptor agonists: arylbenzylimidazole structure-activity relationships. *J Med Chem*. 2006;49(24):7160-7168. doi:10.1021/jm0606185
34. Liu J, Liu Q, Yang X, et al. Design, synthesis, and biological evaluation of 1,2,4-triazole bearing 5-substituted biphenyl-2-sulfonamide derivatives as potential antihypertensive candidates. *Bioorg Med Chem*. 2013;21(24):7742-7751. doi:10.1016/j.bmc.2013.10.017

35. angiotensin II AT(2) receptor agonists with reduced CYP 450 inhibition. *Bioorg Med Chem*. 2010;18(12):4570-4590. doi:10.1016/j.bmc.2010.03.064
36. Wallinder C, Botros M, Rosenström U, et al. Selective angiotensin II AT2 receptor agonists: Benzamide structure-activity relationships. *Bioorg Med Chem*. 2008;16(14):6841-6849. doi:10.1016/j.bmc.2008.05.066
37. Murugaiah a MS, Wallinder C, Mahalingam a K, et al. Selective angiotensin II AT(2) receptor agonists devoid of the imidazole ring system. *Bioorg Med Chem*. 2007;15(22):7166-7183. doi:10.1016/j.bmc.2007.07.026
38. Wallinder C, Sköld C, Botros M, et al. Interconversion of Functional Activity by Minor Structural Alterations in Nonpeptide AT 2 Receptor Ligands. *ACS Med Chem Lett*. 2015;6(2):178-182. doi:10.1021/ml500427r
39. Wannberg J, Isaksson R, Bremberg U, et al. A convenient transesterification method for synthesis of AT2 receptor ligands with improved stability in human liver microsomes. *Bioorg Med Chem Lett*. 2018;28(3):519-522. doi:10.1016/j.bmcl.2017.11.042
40. Isaksson R, Lindman J, Wannberg J, et al. A Series of Analogues to the AT 2 R Prototype Antagonist C38 Allow Fine Tuning of the Previously Reported Antagonist Binding Mode. *ChemistryOpen*. 2019;8(1):114-125. doi:10.1002/open.201800282
41. Wallinder C, Sköld C, Sundholm S, et al. High affinity rigidified AT $_2$ receptor ligands with indane scaffolds. *Medchemcomm*. 2019:2146-2160. doi:10.1039/C9MD00402E
42. Guimond M-O, Wallinder C, Alterman M, Hallberg A, Gallo-Payet N. Comparative functional properties of two structurally similar selective nonpeptide drug-like ligands for the angiotensin II type-2 (AT2) receptor. Effects on neurite outgrowth in NG108-15 cells. *Eur J Pharmacol*. 2013;699(1-3):160-171. doi:10.1016/j.ejphar.2012.11.032
43. Isaksson R, Casselbrant A, Elebring E, Hallberg M, Larhed M, Fändriks L. Direct stimulation of angiotensin II type 2 receptor reduces nitric oxide production in lipopolysaccharide treated mouse macrophages. *Eur J Pharmacol*. 2020;868(October 2019):172855. doi:10.1016/j.ejphar.2019.172855
44. Isaksson R, Kumpiņa I, Larhed M, Wannberg J. Rapid and straightforward transesterification of sulfonyl carbamates. *Tetrahedron Lett*. 2016;57(13):1476-1478. doi:10.1016/j.tetlet.2016.02.071
45. Dudley DT, Panek RL, Major TC, et al. Subclasses of angiotensin II binding sites and their functional significance. *Mol Pharmacol*. 1990;38(3):370-377. http://molpharm.aspetjournals.org/content/38/3/370.long.
46. Nielsen AH, Schauser K, Winther H, Dantzer V, Poulsen K. Angiotensin II receptors and renin in the porcine uterus: myometrial AT2 and endometrial AT1 receptors are down-regulated during gestation. *Clin Exp Pharmacol Physiol*. 1997;24(5):309-314. doi:10.1111/j.1440-1681.1997.tb01193.x
47. Guimond M-O, Hallberg M, Gallo-Payet N, Wallinder C. Saralasin and Sarile Are AT2 Receptor Agonists. *ACS Med Chem Lett*. 2014;5(10):1129-1132. doi:10.1021/ml500278g
48. Wan Y, Wallinder C, Johansson B, et al. First reported nonpeptide AT1 receptor agonist (L-162,313) acts as an AT2 receptor agonist in vivo. *J Med Chem*. 2004;47(6):1536-1546. doi:10.1021/jm031031i
49. Wakchaure PB, Bremberg U, Wannberg J, Larhed M. Synthesis of enantiopure angiotensin II type 2 receptor [AT2R] antagonist EMA401. *Tetrahedron*. 2015;71(38):6881-6887. doi:10.1016/j.tet.2015.07.018
50. Bosnyak S, Welungoda I, Hallberg A, Alterman M, Widdop R, Jones E. Stimulation of angiotensin AT2 receptors by the non-peptide agonist, Compound 21, evokes vasodepressor effects in conscious spontaneously hypertensive rats. *Br J Pharmacol*. 2010;159(3):709-716. doi:10.1111/j.1476-5381.2009.00575.x
51. Ballesteros JA, Weinstein H. Integrated methods for the construction of three-dimensional models and computational probing of structure-function relations in G protein-coupled receptors. In: *Methods in Neurosciences*. Vol 25. Academic Press; 1995:366-428. doi:10.1016/S1043-9471(05)80049-7
52. Houston JB. Utility of in vitro drug metabolism data in predicting in vivo metabolic clearance. *Biochem Pharmacol*. 1994;47(9):1469-1479. doi:10.1016/0006-2952(94)90520-7
53. Obach RS. Prediction of human clearance of twenty-nine drugs from hepatic microsomal intrinsic clearance data: An examination of in vitro half-life approach and nonspecific binding to microsomes. *Drug Metab Dispos*. 1999;27(11):1350-1359.
54. Olander M, Wisniewski JR, Flörkemeier I, Handin N, Urdzik J, Artursson P. A simple approach for restoration of differentiation and function in cryopreserved human hepatocytes. *Arch Toxicol*. 2019;93(3):819-829. doi:10.1007/s00204-018-2375-9
55. Hubatsch I, Ragnarsson EGE, Artursson P. Determination of drug permeability and prediction of drug absorption in Caco-2 monolayers. *Nat Protoc*. 2007;2(9):2111-2119. doi:10.1038/nprot.2007.303
56. Zhang H, Unal H, Gati C, et al. Structure of the Angiotensin Receptor Revealed by Serial Femtosecond Crystallography. *Cell*. 2015;161:833-844. doi:10.1016/j.cell.2015.04.011
57. Zhang H, Han GW, Batyuk A, et al. Structural basis for selectivity and diversity in angiotensin II receptors. *Nature*. 2017;544:327-332. doi:10.1038/nature22035
58. Friesner R a, Banks JL, Murphy RB, et al. Glide: a new approach for rapid, accurate docking and scoring. 1. Method and assessment of docking accuracy. *J Med Chem*. 2004;47(7):1739-1749. doi:10.1021/jm0306430
59. Halgren T a, Murphy RB, Friesner R a, et al. Glide: a new approach for rapid, accurate docking and scoring. 2. Enrichment factors in database screening. *J Med Chem*. 2004;47(7):1750-1759. doi:10.1021/jm030644s
60. Friesner RA, Murphy RB, Repasky MP, et al. Extra Precision Glide: Docking and Scoring Incorporating a Model of Hydrophobic Enclosure for Protein-Ligand Complexes. *J Med Chem*. 2006;49:6177-6196. doi:10.1021/jm051256o
61. Gising J, Odell LR, Larhed M Microwave-Assisted Synthesis of Small Molecules Targeting the Infectious Diseases Tuberculosis, HIV/AIDS, Malaria and Hepatitis C. Org Biomol Chem, 2012;10:2713-2729. doi::10.1039/C2OB06833H
62. Gutiérrez-de-Terán H, Bello X, Rodríguez D. G-Protein-Coupled Receptors: from Structural Insights to Functional Mechanisms Characterization of the dynamic events of GPCRs by automated computational simulations. *Biochem Soc Trans*. 2013;41:205-212. doi:10.1042/BST20120287
63. Esguerra M, Siretskiy A, Bello X, Sallander J, Gutiérrez-de-Terán H. GPCR-ModSim: A comprehensive web based solution for modeling G-protein coupled receptors. *Nucleic Acids Res*. 2016;44:W455-W462. doi:10.1093/nar/gkw403
64. Hess B, Kutzner C, Van Der Spoel D, Lindahl E. GROMACS 4: Algorithms for Highly Efficient, Load-Balanced, and Scalable Molecular Simulation. *J Chem Theory Comput*. 2008;4:435-447. doi:10.1021/ct700301q
65. Kaminski GA, Friesner RA, Tirado-Rives J, Jorgensen WL. Evaluation and Reparametrization of the OPLS-AA Force Field for Proteins via Comparison with Accurate Quantum Chemical Calculations on Peptides. *J Phys Chem B*. 2001;105:6474-6487. doi:10.1021/jp003919d
66. Berger O, Edholm O, Jähnig F. Molecular Dynamics Simulations of a Fluid Bilayer of Dipalmitoylphosphatidylcholine at Full Hydration, Constant Pressure, and Constant Temperature. *Biophys J*. 1997;72:2002-2013. doi:10.1016/S0006-3495(97)78845-3
67. Venkatakrishnan AJ, Deupi X, Lebon G, Tate CG, Schertler GF, Madan Babu M. Molecular signatures of G-protein-coupled receptors. *Nature*. 2013;494:185-194. doi:10.1038/nature11896

Declaration of interests

☒ The authors declare that they have no known competing financial interests or personal relationships that could have appeared to influence the work reported in this paper.

☐The authors declare the following financial interests/personal relationships which may be considered as potential competing interests: